PHILOSOPHICAL TRANSACTIONS OF THE ROYAL SOCIETY A MATHEMATICAL, PHYSICAL & ENGINEERING SCIENCES

Stabilizing and destabilizing perturbations of -symmetric indefinitely damped systems

O. N. Kirillov

Phil. Trans. R. Soc. A 2013 **371**, 20120051, published 18 March 2013

PHILOSOPHICAL TRANSACTIONS OF THE ROYAL SOCIETY A

rsta.royalsocietypublishing.org

Research

Cite this article: Kirillov ON. 2013 Stabilizing and destabilizing perturbations of $\mathcal{PT}$-symmetric indefinitely damped systems. Phil Trans R Soc A 371: 20120051.
http://dx.doi.org/10.1098/rsta.2012.0051

One contribution of 17 to a Theme Issue '$\mathcal{PT}$ quantum mechanics'.

Subject Areas:
mathematical physics, wave motion, applied mathematics, mechanics, fluid mechanics

Keywords:
indefinite damping, $\mathcal{PT}$-symmetry, Krein signature, dissipation-induced instabilities, exceptional point, modulational instability

Author for correspondence:
O. N. Kirillov
e-mail: o.kirillov@hzdr.de

Royal Society Publishing
Informing the science of the future

Stabilizing and destabilizing perturbations of $\mathcal{PT}$-symmetric indefinitely damped systems

O. N. Kirillov

Helmholtz-Zentrum Dresden-Rossendorf, FWDH, PO Box 510119, 01314 Dresden, Germany

Eigenvalues of a potential dynamical system with damping forces that are described by an indefinite real symmetric matrix can behave as those of a Hamiltonian system when gain and loss are in a perfect balance. This happens when the indefinitely damped system obeys parity–time ($\mathcal{PT}$) symmetry. How do pure imaginary eigenvalues of a stable $\mathcal{PT}$-symmetric indefinitely damped system behave when variation in the damping and potential forces destroys the symmetry? We establish that it is essentially the tangent cone to the stability domain at the exceptional point corresponding to the Whitney umbrella singularity on the stability boundary that manages transfer of instability between modes.

1. Introduction

The notion of *indefinite damping* has originated in the problems of stability of solutions to the wave equation [1,2]

$$u_{tt} + \varepsilon a(x) u_t = u_{xx}, \tag{1.1}$$

where the damping coefficient $a(x)$ is assumed to be a function changing its sign in the interval $x \in (0,1)$. Such problems arise, for example, in structural dynamics where the viscous damping material distributed over part of the vibrating structure can be used to control the vibration [3]. It turns out that for any sign-changing damping distribution $a(x)$, there exists $\varepsilon_0 > 0$, such that for all $0 < \varepsilon < \varepsilon_0$, the trivial solution of (1.1) is asymptotically stable, i.e. it is decaying with time [2]. The dependence of ε_0 on a is however very non-trivial. In order to understand it better, Freitas *et al.* [4] formulated a finite-dimensional version of problem (1.1)

$$\ddot{\mathbf{u}} + \varepsilon \mathbf{A}\dot{\mathbf{u}} = \mathbf{B}\mathbf{u}, \tag{1.2}$$

where the dot is time differentiation, $\mathbf{u} \in \mathbb{R}^n$, $\mathbf{B}$ is a real diagonal matrix and $\mathbf{A} = \mathbf{A}^{\mathrm{T}}$ is a real indefinite matrix. As an illustration of the sensitivity of ε_0 to the entries of the matrices, Freitas *et al.* [4] considered the following two-dimensional example: $a_{11} = 1, a_{12} = 1, a_{22} = \frac{1}{2}$ and $b_{11} = -1$, $b_{22} = -4, b_{12} = 0$. Then, $\varepsilon_0 \simeq 1.15$. However, an interchange of the diagonal entries of the matrix $\mathbf{B}$ leads to an increase in the interval of the asymptotic stability: $\varepsilon_0 \simeq 1.41$.

Nevertheless, even the instability threshold found in Freitas *et al.* [4] for a two-degrees-of-freedom system (1.2) did not lead to a clear interpretation that would explain the 'wild' dependence of ε_0 on the matrices of potential and damping forces. Furthermore, a subsequent investigation made in Freitas [5] revealed an intriguing fact that with specifically chosen matrices $\mathbf{A}$ and $\mathbf{B}$, the eigenvalues of the system (1.2) behave like those of a Hamiltonian system, as they are located symmetrical to both the real and imaginary axes of the complex plane. Such an *oscillatory-damped system* [5] is marginally stable when $0 < \varepsilon < \varepsilon_0$ with all its eigenvalues pure imaginary and simple, which corresponds to the bounded oscillations. The oscillations become unstable (flutter) when $\varepsilon \geq \varepsilon_0$.

More precisely, the spectrum of equation (1.2) has a Hamiltonian symmetry, if and only if there exists a matrix $\mathbf{T}$ such that $\mathbf{TAT} = -\mathbf{A}$. If, additionally, the diagonal matrix $-\mathbf{B} > 0$, then the solutions of equation (1.2) are bounded for ε in a neighbourhood of the origin that depends on $\mathbf{A}$ and $\mathbf{B}$ [5].

As an example, let us consider an equation $\ddot{\mathbf{q}} + \varepsilon\tilde{\mathbf{A}}\dot{\mathbf{q}} = \tilde{\mathbf{B}}\mathbf{q}$ with the matrices

$$\tilde{\mathbf{A}} = \begin{pmatrix} -1 & 0 \\ 0 & 1 \end{pmatrix} \quad \text{and} \quad \tilde{\mathbf{B}} = \frac{1}{1-\mu^2}\begin{pmatrix} -1 & \mu \\ \mu & -1 \end{pmatrix}, \tag{1.3}$$

which describes two coupled ideal LRC circuits, i.e. electrical circuits consisting of inductors, resistors and capacitors, one with gain (realized by means of the voltage amplifier) and another with loss (resistance), where $0 < \mu < 1$ is the mutual inductance and $\varepsilon > 0$ is loss that perfectly matches the gain $(-\varepsilon)$. The components of the vector $\mathbf{q}$, i.e. q_1 and q_2, are indeed charges on the capacitors of the electric circuit [6]. A coordinate transformation by means of the matrix $\mathbf{C}$ reduces this equation to the form (1.2) with $\mathbf{B} = \mathbf{C}\tilde{\mathbf{B}}\mathbf{C}^{-1}$ and $\mathbf{A} = \mathbf{C}\tilde{\mathbf{A}}\mathbf{C}^{-1}$, where

$$\mathbf{A} = \begin{pmatrix} 0 & -1 \\ -1 & 0 \end{pmatrix}, \quad \mathbf{B} = \begin{pmatrix} \dfrac{1}{\mu-1} & 0 \\ 0 & \dfrac{-1}{\mu+1} \end{pmatrix} \quad \text{and} \quad \mathbf{C} = \begin{pmatrix} 1 & -1 \\ 1 & 1 \end{pmatrix}. \tag{1.4}$$

Because $\mathbf{TAT} = -\mathbf{A}$ with $\mathbf{T} = \mathrm{diag}(1, -1)$, the spectrum of the two coupled LRC circuits with perfectly matched gain and loss considered in Schindler *et al.* [6] is Hamiltonian. When $0 < \varepsilon < \varepsilon_0 = 1/\sqrt{1-\mu} - 1/\sqrt{1+\mu}$, the system is marginally stable, i.e. it is the oscillatory-damped system in terms of Freitas [5].

On the other hand, Schindler *et al.* [6] pointed out that their equations with the matrices (1.3) are invariant under a combined *parity* ($q_1 \leftrightarrow q_2$) and *time-reversal* ($t \leftrightarrow -t$) transformation. This immediately connects the 'oscillatory-damped systems' of Freitas [5] to the fundamental $\mathcal{PT}$*-symmetry* [7–9].

The notion of $\mathcal{PT}$-symmetry entered modern physics mainly from the quantum mechanics aspect. Parametric families of non-Hermitian Hamiltonians having both parity ($\mathcal{P}$) and time-reversal ($\mathcal{T}$) symmetry possess a pure real spectrum in some regions of the parameter space, which questions the need for the Hermiticity axiom in quantum theory [7,10,11]. First experimental evidence of $\mathcal{PT}$-symmetry came, however, from classical optics [12], where the properly designed imaginary part of the linear refractive index yields inhomogeneous space gain and loss[1] [13]. The recently designed experiment with the $\mathcal{PT}$-symmetric LRC circuits can be regarded as an analogue model of the optical systems [6].

$\mathcal{PT}$-symmetric nonlinear gain and loss that signs can be periodically switched were proposed to stabilize the localized solutions (solitons) in two coupled perturbed nonlinear Schrödinger equations (NLS) [14,15]. It is known, however, that stable pulses in the dual-core systems of

[1]This reminds us of the placement of dampers and actuators in engineering problems of vibration control [3].

nonlinear optics frequently exist far from the $\mathcal{PT}$-symmetry conditions that provide a perfect matching of gain and loss [16,17]. This may indicate that the challenging problem of finding stability conditions for such solitons [16,17] has connections with the question on the dependency of the instability threshold of a potential system with the general indefinite damping matrix raised by Freitas *et al.* [4]. In any case, in real electric circuits, it should be easy to introduce additional losses in order to model departure from the ideal $\mathcal{PT}$-symmetric system considered in Schindler *et al.* [6] and, thus experimentally understand the effect of indefinite damping in more detail.

Taking into account commercial availability of Tellegen's gyrators that introduce gyroscopic effects in LRC circuits [18], the experiment described in Schindler *et al.* [6] could be extended in order to study stability of gyroscopic systems with indefinite damping. The latter arise in mechanical engineering applications that deal with instabilities in rotating and moving media induced by dry friction. A common singing wine glass provides an example [19]. Indeed, the dependence of the friction coefficient of a finger applied to a rotating wine glass on the velocity of rotation has a negative slope [20]. The latter produces negative damping coefficients in the linearized equations of motion, which can be interpreted as a sort of 'gain' [21]. Together with viscous losses, these terms result in the indefinite damping matrix that perturbs a gyroscopic system [22]. Note that in such systems, a non-trivial choice of matrices of damping and potential forces is possible, which implies the Hamiltonian symmetry of the spectrum [23].

2. Potential system with indefinite damping

Consider a linear potential system with n degrees of freedom,

$$\ddot{\mathbf{z}} + \mathbf{D}\dot{\mathbf{z}} + \mathbf{K}\mathbf{z} = 0, \tag{2.1}$$

where the dot stands for time differentiation, and the real matrix of potential forces is $\mathbf{K} = \mathbf{K}^{\mathrm{T}} > 0$. The real matrix $\mathbf{D} = \mathbf{D}^{\mathrm{T}}$ of the damping forces is assumed to be indefinite, i.e. its spectrum contains both positive and negative real eigenvalues [4]. Such a system appeared, for example, in a recent study of two coupled LRC circuits, one with gain and another one with loss, see Schindler *et al.* [6].

Assuming the solutions to equation (2.1) in the form $\mathbf{z} \sim \mathbf{u}\exp(\lambda t)$, we obtain the eigenvalue problem for a matrix polynomial,

$$\mathbf{L}_1(\lambda)\mathbf{u} := (\lambda^2 + \mathbf{D}\lambda + \mathbf{K})\mathbf{u} = 0. \tag{2.2}$$

When $n = 2$, the Leverrier–Barnett algorithm [24] applied to $\mathbf{L}_1$ results in the characteristic polynomial

$$p(\lambda) = \lambda^4 + p_1\lambda^3 + p_2\lambda^2 + p_3\lambda + p_4, \tag{2.3}$$

with the coefficients

$$\left.\begin{aligned} &p_1 = \mathrm{tr}\mathbf{D}, \quad p_2 = \mathrm{tr}\mathbf{K} + \det\mathbf{D}, \\ &p_3 = \mathrm{tr}\mathbf{K}\mathrm{tr}\mathbf{D} - \mathrm{tr}\mathbf{K}\mathbf{D} \quad \text{and} \quad p_4 = \det\mathbf{K}. \end{aligned}\right\} \tag{2.4}$$

Denoting $\Upsilon = \delta_2 - \delta_1$ as a difference between the eigenvalues δ_1 and δ_2 of $\mathbf{D}$, we find

$$\det\mathbf{D} = \tfrac{1}{4}((\mathrm{tr}\mathbf{D})^2 - \Upsilon^2). \tag{2.5}$$

Given $\mathbf{K}$, let $\mathbf{D}_{\mathcal{PT}}$ be a matrix satisfying the equalities

$$\mathrm{tr}\mathbf{D}_{\mathcal{PT}} = 0 \quad \text{and} \quad \mathrm{tr}\mathbf{K}\mathbf{D}_{\mathcal{PT}} = 0. \tag{2.6}$$

Then, in equation (2.3), the coefficients p_1 and p_3 vanish, $\det\mathbf{D}_{\mathcal{PT}} = -\Upsilon_{\mathcal{PT}}^2/4 < 0$, and the eigenvalues can be found explicitly as

$$\lambda_{\mathcal{PT}}^2 = -\frac{\mathrm{tr}\mathbf{K}}{2} + \frac{\Upsilon_{\mathcal{PT}}^2}{8} \pm \frac{1}{8}\sqrt{((\Upsilon_{\mathcal{PT}})^2 - (\Upsilon_{\mathcal{PT}}^-)^2)((\Upsilon_{\mathcal{PT}})^2 - (\Upsilon_{\mathcal{PT}}^+)^2)}, \tag{2.7}$$

where

$$\Upsilon_{\mathcal{PT}}^{\pm} = 2(\sqrt{\kappa_2} \pm \sqrt{\kappa_1}), \tag{2.8}$$

κ_1 and κ_2 are the eigenvalues of the matrix $\mathbf{K}$.

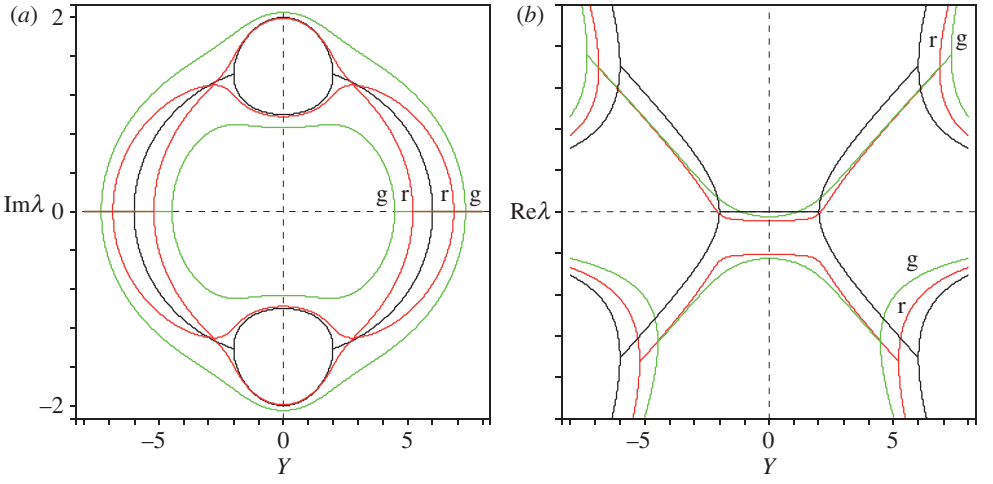

Figure 1. For $\kappa_1 = 1$ and $\kappa_2 = 4$: (*a*) imaginary and (*b*) real parts of the eigenvalues of the system (2.1) versus $Y = \delta_1 - \delta_2$ when (black) tr**D** = 0 and tr**KD** = 0 ($\mathcal{PT}$-symmetric system), (green, g) tr**D** = 1, and tr**KD** = 1.1 and (red, r) tr**D** = 1 and tr**KD** = 3.5. (Online version in colour.)

Imaginary and real parts of eigenvalues $\lambda_{\mathcal{PT}}$ given by equation (2.7) as functions of $Y = Y_{\mathcal{PT}}$ are represented in figure 1 as black curves in the particular case when $\kappa_1 = 1$ and $\kappa_2 = 4$. The eigenvalues are simple and pure imaginary for $Y^2 < (Y^-_{\mathcal{PT}})^2$. At $Y^2 = (Y^-_{\mathcal{PT}})^2$, the eigenvalues pass through the non-semisimple 1 : 1 resonance and originate a double pure imaginary eigenvalue with the Jordan block. Thus, the values $\pm Y^-_{\mathcal{PT}}$ are exceptional points (EPs) [25] of the parameter Y. When Y^2 exceeds $(Y^-_{\mathcal{PT}})^2$, the eigenvalues become complex with positive and negative real parts, which means oscillatory instability or flutter. Further increases in Y^2 result in the merging of complex-conjugate eigenvalues into double real ones at $\pm Y^+_{\mathcal{PT}}$, which then split into simple real eigenvalues (divergence or static instability; figure 1).

Therefore, the spectrum of the system (2.1) with the indefinite damping matrix $\mathbf{D}_{\mathcal{PT}}$ is Hamiltonian, i.e. the eigenvalues are symmetric with respect to both real and imaginary axes of the complex plane [5]. To illustrate this, we choose

$$\mathbf{K} = \frac{1}{2}\begin{pmatrix} 5-\sqrt{5} & 2 \\ 2 & 5+\sqrt{5} \end{pmatrix} \quad \text{and} \quad \mathbf{D}_{\mathcal{PT}} = \frac{Y}{6}\begin{pmatrix} 2 & \sqrt{5} \\ \sqrt{5} & -2 \end{pmatrix}. \tag{2.9}$$

The matrix **K** has eigenvalues $\kappa_1 = 1$ and $\kappa_2 = 4$. The eigenvalues of $\mathbf{D}_{\mathcal{PT}}$ are $\delta_1 = -Y/2$ and $\delta_2 = Y/2$. Then, the characteristic polynomial (2.3) takes the form

$$p(\lambda) = \lambda^4 + \left(5 - \frac{Y^2}{4}\right)\lambda^2 + 4. \tag{2.10}$$

The real and imaginary parts of its roots are shown in figure 1 as black curves.

Expressing the components d_{12} and d_{22} of the matrix **D** from the conditions (2.6) where we assume that $k_{12} \neq 0$ and then changing coordinates as $x_1 = z_1 + \mathrm{i}z_2$, $x_2 = \bar{x}_1$, $x_3 = \dot{x}_1$, $x_4 = \dot{x}_2$, where $\mathrm{i} = \sqrt{-1}$ and the overbar denotes complex conjugation, we transform equation (2.1) to $\mathrm{i}\dot{\mathbf{x}} = \mathbf{H}\mathbf{x}$, where

$$\mathbf{H} = \begin{pmatrix} 0 & 0 & \mathrm{i} & 0 \\ 0 & 0 & 0 & \mathrm{i} \\ -\mathrm{i}\dfrac{k_{11}+k_{22}}{2} & k_{12} - \mathrm{i}\dfrac{k_{11}-k_{22}}{2} & 0 & d_{11}\dfrac{k_{22}-k_{11}}{2k_{12}} - \mathrm{i}d_{11} \\ -k_{12} - \mathrm{i}\dfrac{k_{11}-k_{22}}{2} & -\mathrm{i}\dfrac{k_{11}+k_{22}}{2} & -d_{11}\dfrac{k_{22}-k_{11}}{2k_{12}} - \mathrm{i}d_{11} & 0 \end{pmatrix}. \tag{2.11}$$

For example, when $k_{11}=k_{22}$, we have $\mathbf{P}\bar{\mathbf{H}}^{\mathrm{T}}=\mathbf{H}\mathbf{P}$, where $\mathbf{P}=\mathrm{diag}(1,-1,-1,1)$ [26], that is, in this particular case, $\mathbf{H}$ is a $\mathcal{PT}$-symmetric non-Hermitian Hamiltonian [8,9] that contains, for example, the model considered by Schindler *et al.* [6].

Is $\mathbf{H}$ in (2.11) $\mathcal{PT}$-symmetric also when $k_{11}\neq k_{22}$? We leave this as an open question. Because the spectrum of i$\mathbf{H}$ has the Hamiltonian symmetry, we will keep the subscript $\mathcal{PT}$ in the notation when we deal with the matrices satisfying the conditions (2.6).

The Hamiltonian symmetry of the spectrum of the indefinitely damped system is lost when the matrices $\mathbf{D}$ and $\mathbf{K}$ do not satisfy the conditions (2.6). In this case, system (2.1) can be asymptotically stable if and only if the coefficients (2.4) of the characteristic polynomial fulfil the criteria of Routh and Hurwitz: $p_1>0$, $p_2>0$, $p_4>0$ and $p_1p_2p_3-p_1^2p_4-p_3^2>0$. Because we assumed that $\mathbf{K}>0$, the conditions for asymptotic stability are reduced to $\mathrm{tr}\mathbf{D}>0$ and [4,27]

$$Y^2>(\mathrm{tr}\mathbf{D})^2+4\frac{(\mathrm{tr}\mathbf{K}\mathbf{D}-\kappa_1\mathrm{tr}\mathbf{D})(\mathrm{tr}\mathbf{K}\mathbf{D}-\kappa_2\mathrm{tr}\mathbf{D})}{\mathrm{tr}\mathbf{D}(\mathrm{tr}\mathbf{K}\mathbf{D}-\mathrm{tr}\mathbf{K}\mathrm{tr}\mathbf{D})}. \tag{2.12}$$

In order to get an idea how the new instability threshold (2.12) is related to that of the indefinitely damped system with the Hamiltonian symmetry of the spectrum, $Y^2<(Y^-_{\mathcal{PT}})^2$, we express the coefficients of the polynomial $p(\lambda)$ by means of Y and $Y^{\pm}_{\mathcal{PT}}$ as

$$\left.\begin{aligned} p_2&=\frac{(Y^-_{\mathcal{PT}})^2+(Y^+_{\mathcal{PT}})^2+2(\mathrm{tr}\mathbf{D}^2-Y^2)}{8},\\ p_3&=\frac{(Y^-_{\mathcal{PT}})^2+(Y^+_{\mathcal{PT}})^2}{8}\mathrm{tr}\mathbf{D}-\mathrm{tr}\mathbf{K}\mathbf{D}\quad\text{and}\quad p_4=\left(\frac{(Y^+_{\mathcal{PT}})^2-(Y^-_{\mathcal{PT}})^2}{16}\right)^2. \end{aligned}\right\} \tag{2.13}$$

Plotting the real and imaginary parts of the eigenvalues versus the parameter Y at different values of $\mathrm{tr}\mathbf{D}\neq 0$ and $\mathrm{tr}\mathbf{K}\mathbf{D}\neq 0$ for a given $\mathbf{K}$, we observe that the perturbed eigenvalues are complex, as demonstrated by the green ('g') and red ('r') lines in figure 1. Note that the unfolding of the 1 : 1 resonance happens in such a manner that the imaginary parts avoid crossing for relatively small values of $\mathrm{tr}\mathbf{K}\mathbf{D}$ (g lines in figure 1*a*) and cross when $\mathrm{tr}\mathbf{K}\mathbf{D}$ takes larger values (r lines in figure 1*a*). This means that in the former case, the mode with the higher frequency of oscillations becomes unstable, whereas in the latter, instability transfers from the higher frequency mode to the lower frequency one.

Another effect of the violation of the conditions (2.6) is that the real parts of the eigenvalues become positive either at (r lines) higher or (g lines) lower values of Y than the threshold $Y^-_{\mathcal{PT}}$, figure 1*b*. The latter means shrinking the interval of stability with respect to that of the oscillatory-damped system. Moreover, to maintain the ratio of $\mathrm{tr}\mathbf{K}\mathbf{D}$ and $\mathrm{tr}\mathbf{D}$ constant and tend, e.g. $\mathrm{tr}\mathbf{D}$ to zero, then the limiting stability interval will not coincide with that of an oscillatory-damped system demonstrating a discontinuity between the two thresholds of instability (known as the *Ziegler–Bottema destabilization paradox* [28–30]).

Assuming equality in equation (2.12), we resolve it with respect to $\mathrm{tr}\mathbf{K}\mathbf{D}$ and write the threshold of asymptotic stability in the form

$$\begin{aligned}\mathrm{tr}\mathbf{K}\mathbf{D}=&\frac{(Y^-_{\mathcal{PT}})^2+(Y^+_{\mathcal{PT}})^2}{16}\mathrm{tr}\mathbf{D}\\&+\frac{\mathrm{tr}\mathbf{D}}{8}\left[Y^2-(\mathrm{tr}\mathbf{D})^2\pm\sqrt{(Y^2-(\mathrm{tr}\mathbf{D})^2-(Y^-_{\mathcal{PT}})^2)(Y^2-(\mathrm{tr}\mathbf{D})^2-(Y^+_{\mathcal{PT}})^2)}\right].\end{aligned} \tag{2.14}$$

Two sheets of the surface (2.14), corresponding to different signs before the square root, intersect each other along an interval of the Y-axis in the $(\mathrm{tr}\mathbf{D},\mathrm{tr}\mathbf{K}\mathbf{D},Y)$ space, figure 2*a*. When

$$Y^2=(Y^-_{\mathcal{PT}})^2+(\mathrm{tr}\mathbf{D})^2, \tag{2.15}$$

the two sheets are connected along a space curve that projects into a straight line,

$$\mathrm{tr}\mathbf{K}\mathbf{D}=\frac{\mathrm{tr}\mathbf{D}}{16}(3(Y^-_{\mathcal{PT}})^2+(Y^+_{\mathcal{PT}})^2), \tag{2.16}$$

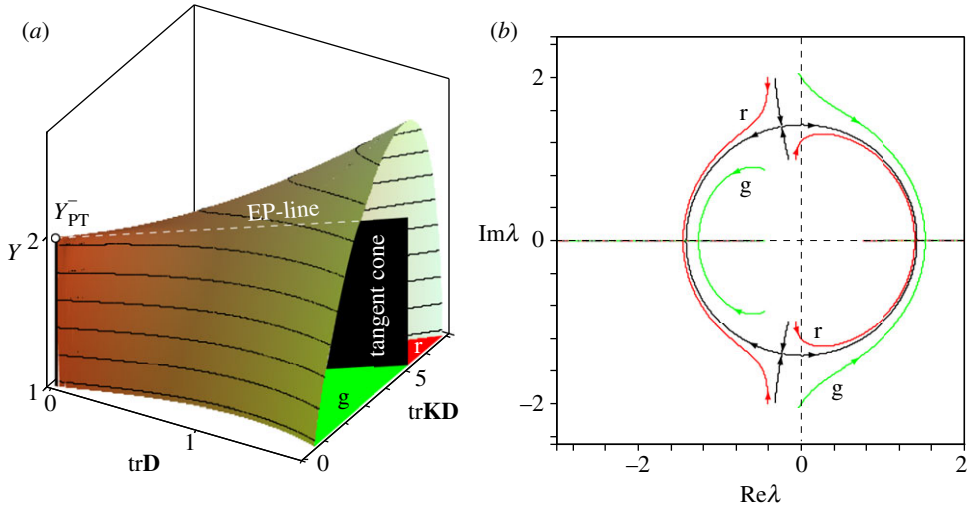

Figure 2. When $\kappa_1 = 1$ and $\kappa_2 = 4$: (*a*) in the half-space $\mathrm{tr}\mathbf{D} > 0$ of the $(\mathrm{tr}\mathbf{D}, \mathrm{tr}\mathbf{KD}, Y)$ space, where $Y = \delta_1 - \delta_2$, a part of the surface (2.14) with the Whitney umbrella singularity at the EP $(0, 0, Y^-_{\mathcal{PT}})$ bounds the domain of asymptotic stability of the indefinitely damped system (2.1). The tangent cone $\{\mathrm{tr}\mathbf{KD} = \mathrm{tr}\mathbf{D}(\mathrm{tr}\mathbf{K} - \sqrt{\det \mathbf{K}}), Y < Y^-_{\mathcal{PT}}, \mathrm{tr}\mathbf{D} > 0\}$ to the stability domain at $(0, 0, Y^-_{\mathcal{PT}})$ is shown in black. At the points of the (white dashed) EP line $\{\mathrm{tr}\mathbf{KD} = \mathrm{tr}\mathbf{D}(\mathrm{tr}\mathbf{K} - \sqrt{\det \mathbf{K}}), Y = Y^-_{\mathcal{PT}}\}$, the eigenvalues of the system (2.1) are double non-semisimple. (*b*) Movement of eigenvalues of the system (2.1) when Y varies from 0 to 8 and (black) $\mathrm{tr}\mathbf{D} = 1$ and $\mathrm{tr}\mathbf{KD} = 3$, (green, g) $\mathrm{tr}\mathbf{D} = 1$ and $\mathrm{tr}\mathbf{KD} = 1.1$, and (red, r) $\mathrm{tr}\mathbf{D} = 1$ and $\mathrm{tr}\mathbf{KD} = 3.5$. It illustrates how penetrating the tangent cone yields exchange of instability between modes. (Online version in colour.)

lying in the $(\mathrm{tr}\mathbf{D}, \mathrm{tr}\mathbf{KD})$ plane. According to equation (2.15), the space curve lying on the surface (2.14) passes through the point $Y = Y^-_{\mathcal{PT}}$ when $\mathrm{tr}\mathbf{D} = 0$. Therefore, the interval of self-intersection is determined by the inequality $Y^2 \leq (Y^-_{\mathcal{PT}})^2$, which contains the interval of marginal stability $Y^2 < (Y^-_{\mathcal{PT}})^2$ of the oscillatory-damped system, figure 2*a*. Retaining only the terms of order $O(\mathrm{tr}\mathbf{D})$ in equation (2.14), we obtain a linear approximation to the intersecting sheets at the points of the interval $Y^2 \leq (Y^-_{\mathcal{PT}})^2$ of the y-axis,

$$\mathrm{tr}\mathbf{KD} = \frac{\mathrm{tr}\mathbf{D}}{16}\left[(Y^-_{\mathcal{PT}})^2 + (Y^+_{\mathcal{PT}})^2 + 2Y^2 \pm 2\sqrt{(Y^2 - (Y^-_{\mathcal{PT}})^2)(Y^2 - (Y^+_{\mathcal{PT}})^2)}\right]. \tag{2.17}$$

Near the line (2.16) in the neighbourhood of the EP $(\mathrm{tr}\mathbf{D} = 0, \mathrm{tr}\mathbf{KD} = 0, Y = Y^-_{\mathcal{PT}})$, the linear approximation (2.17) yields a simple estimate of the instability threshold,

$$Y \simeq Y^-_{\mathcal{PT}} - \frac{(32\mathrm{tr}\mathbf{KD} - 2(3(Y^-_{\mathcal{PT}})^2 + (Y^+_{\mathcal{PT}})^2)\mathrm{tr}\mathbf{D})^2}{Y^-_{\mathcal{PT}}|(Y^-_{\mathcal{PT}})^2 - (Y^+_{\mathcal{PT}})^2|(\mathrm{tr}\mathbf{D})^2}. \tag{2.18}$$

Note that equation (2.18) is in the form $Y = X^2/Z^2$, which is canonical for the Whitney umbrella surface [31]. Therefore, the surface (2.14) contains the Whitney umbrella singularity at the EP $(0, 0, Y^-_{\mathcal{PT}})$ of the $(\mathrm{tr}\mathbf{D}, \mathrm{tr}\mathbf{KD}, Y)$ space, which is a generic singularity of codimension 3 on the boundary of asymptotic stability of a general family of real matrices [31] that is associated with the double pure imaginary eigenvalue with the Jordan block [29,32,33].

A pocket of the singular surface (2.14) selected by the condition $\mathrm{tr}\mathbf{D} > 0$ bounds the domain of asymptotic stability of the indefinitely damped system (2.1). The part of the plane (2.16) in the $(\mathrm{tr}\mathbf{D}, \mathrm{tr}\mathbf{KD}, Y)$ space under the constraints $\mathrm{tr}\mathbf{D} > 0$ and $Y < Y^-_{\mathcal{PT}}$ constitutes the tangent cone to the stability domain at the EP [34,35]. This tangent cone touching the stability boundary at the EP is shown in black in figure 2*a*. It separates the stability pocket into the 'green' and 'red' compartments marked also by, respectively, the letters 'g' and 'r' in figure 2*a*. Below, we will show that this subdivision controls the eigenvalue movement in the complex plane [36].

We first observe that the upper bound to the tangent cone, i.e. the ray specified by the expressions (2.16), $Y = Y^{-}_{\mathcal{PT}}$ and $\mathrm{tr}\mathbf{D} > 0$, consists of the EPs. Indeed, the spectrum of the system (2.1) with $n = 2$ degrees of freedom at the points of the ray shown as a white dashed line in figure 2*a* consists of a pair of double complex-conjugate eigenvalues,

$$\lambda = -\frac{1}{4}\mathrm{tr}\mathbf{D} \pm \frac{\mathrm{i}}{4}\sqrt{(Y^{+}_{\mathcal{PT}})^2 - (Y^{-}_{\mathcal{PT}})^2 - (\mathrm{tr}\mathbf{D})^2}. \tag{2.19}$$

The pair (2.19) lives in the complex plane on the circle

$$(\mathrm{Re}\lambda)^2 + (\mathrm{Im}\lambda)^2 = \frac{(Y^{+}_{\mathcal{PT}})^2 - (Y^{-}_{\mathcal{PT}})^2}{16}. \tag{2.20}$$

When Y increases within the black tangent cone in figure 2*a*, $\mathrm{tr}\mathbf{D}$ and $\mathrm{tr}\mathbf{KD}$ fixed, two simple complex eigenvalues $\lambda(Y)$ are attracted to an EP on the circle (2.20) that is shown in black in figure 2*b*. They merge at an EP into a double eigenvalue with a negative real part when $Y = Y^{-}_{\mathcal{PT}}$. After its subsequent splitting, the newborn simple eigenvalues evolve along the circle (2.20) in opposite directions, figure 2*b*. At the instability threshold (2.15), the eigenvalues are

$$\lambda = \pm\frac{\mathrm{i}}{4}\sqrt{(Y^{+}_{\mathcal{PT}})^2 - (Y^{-}_{\mathcal{PT}})^2} \quad \text{and} \quad \lambda = -\frac{1}{2}\mathrm{tr}\mathbf{D} \pm \frac{\mathrm{i}}{4}\sqrt{(Y^{+}_{\mathcal{PT}})^2 - (Y^{-}_{\mathcal{PT}})^2 - 4(\mathrm{tr}\mathbf{D})^2}. \tag{2.21}$$

When Y exceeds the threshold (2.15), the first pair of eigenvalues moves in the complex plane to the right from the imaginary axis, causing instability. The described behaviour of the eigenvalues remarkably reminds us of the movement of Floquet multipliers in a Krein collision [37].

Choosing $\mathrm{tr}\mathbf{D}$ and $\mathrm{tr}\mathbf{KD}$ aside from the tangent cone destroys the perfect collision of eigenvalues on the circle (2.20), as demonstrated by the green (g) and red (r) eigencurves in figure 2*b* corresponding to the parameters taken, respectively, from the 'green' or 'red' compartment of the stability domain shown in figure 2*a*. When the parameters are in the g area selected by the condition $\mathrm{tr}\mathbf{KD} < \mathrm{tr}\mathbf{D}/16(3(Y^{-}_{\mathcal{PT}})^2 + (Y^{+}_{\mathcal{PT}})^2)$, the eigenvalues do not interact and pass in close vicinity of the EP in such a manner that the mode with the higher frequency destabilizes the system, figure 2*b*. When $\mathrm{tr}\mathbf{KD} > \mathrm{tr}\mathbf{D}/16(3(Y^{-}_{\mathcal{PT}})^2 + (Y^{+}_{\mathcal{PT}})^2)$, the black eigencurves in figure 2*b* unfold into two red ones. In this case, the instability transfers to the mode with the lower frequency.

To illustrate our geometrical considerations, let us study the stability of the system (2.1) with the following matrices of potential forces and indefinite damping:

$$\left.\begin{aligned} &\mathbf{K} = \begin{pmatrix} 1 & 0 \\ 0 & 4 \end{pmatrix}, \quad \mathbf{D}_{\mathrm{b}} = \frac{1}{3}\begin{pmatrix} 1 & \sqrt{11} \\ \sqrt{11} & 2 \end{pmatrix} \\ &\mathbf{D}_{\mathrm{r}} = \frac{1}{6}\begin{pmatrix} 1 & \sqrt{41} \\ \sqrt{41} & 5 \end{pmatrix} \quad \text{and} \quad \mathbf{D}_{\mathrm{g}} = \frac{1}{30}\begin{pmatrix} 29 & \sqrt{929} \\ \sqrt{929} & 1 \end{pmatrix}. \end{aligned}\right\} \tag{2.22}$$

The eigenvalues of the matrix $\mathbf{K}$ are $\kappa_1 = 1$ and $\kappa_2 = 4$. The damping matrices are isospectral, i.e. all the three indefinite damping matrices have as eigenvalues

$$\delta_1 = \tfrac{1}{2}(1 - \sqrt{5}) < 0 \quad \text{and} \quad \delta_2 = \tfrac{1}{2}(1 + \sqrt{5}) > 0. \tag{2.23}$$

Then, $\mathrm{tr}\mathbf{D}_{\mathrm{b}} = \mathrm{tr}\mathbf{D}_{\mathrm{g}} = \mathrm{tr}\mathbf{D}_{\mathrm{r}} = 1$. However, $\mathrm{tr}\mathbf{KD}_{\mathrm{b}} = 3$, $\mathrm{tr}\mathbf{KD}_{\mathrm{r}} = 3.5$ and $\mathrm{tr}\mathbf{KD}_{\mathrm{g}} = 1.1$. Therefore, the matrix $\mathbf{D}_{\mathrm{b}}$ corresponds to the black tangent cone in figure 2*a*, $\mathbf{D}_{\mathrm{g}}$ to the green compartment of the stability domain, and $\mathbf{D}_{\mathrm{r}}$ to the red one.

Calculating the eigenvalues λ of the eigenvalue problem (2.2) with the three damping matrices and the matrix $\mathbf{K}$ from equation (2.22), we find

$$\left.\begin{aligned} &\lambda^{\mathrm{b}}_1 = -\frac{1}{2} \pm \mathrm{i}\frac{\sqrt{7}}{2}, \quad \lambda^{\mathrm{b}}_2 = \pm\mathrm{i}\sqrt{2}, \\ &\lambda^{\mathrm{g}}_1 \simeq -0.672 \pm \mathrm{i}0.889, \quad \lambda^{\mathrm{g}}_2 \simeq 0.172 \pm \mathrm{i}1.786, \\ &\lambda^{\mathrm{r}}_1 \simeq -0.548 \pm \mathrm{i}1.489 \quad \text{and} \quad \lambda^{\mathrm{r}}_2 \simeq 0.048 \pm \mathrm{i}1.260. \end{aligned}\right\} \tag{2.24}$$

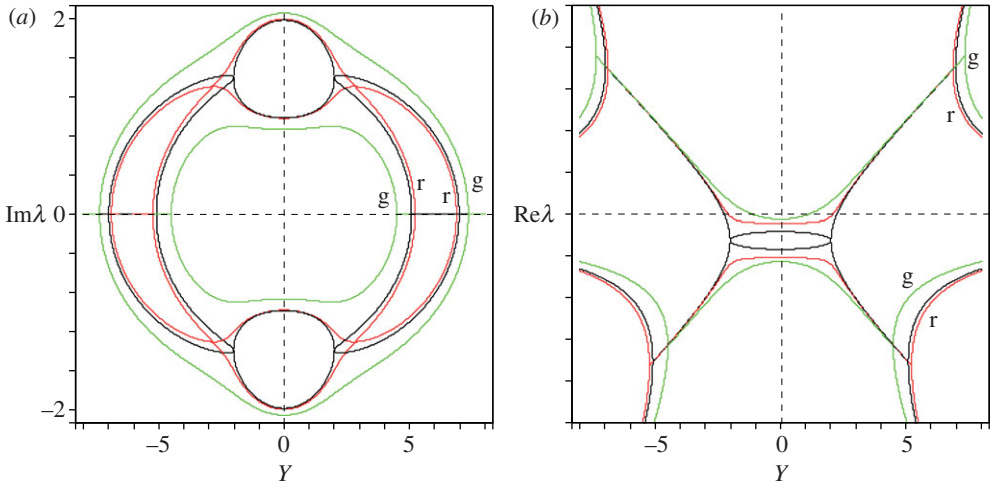

Figure 3. For $\kappa_1 = 1$ and $\kappa_2 = 4$: (*a*) imaginary and (*b*) real parts of the eigenvalues of the system (2.1) versus $Y = \delta_1 - \delta_2$ when (black) tr$\mathbf{D} = 1$ and tr$\mathbf{KD} = 3$ (tangent cone), (green, g) tr$\mathbf{D} = 1$ and tr$\mathbf{KD} = 1.1$, and (red, r) tr$\mathbf{D} = 1$ and tr$\mathbf{KD} = 3.5$. (Online version in colour.)

Thus, system (2.1) with the indefinite damping matrix $\mathbf{D}_\mathrm{b}$ is exactly at the stability boundary that, according to equation (2.15), corresponds to $Y = \sqrt{5}$. At the same $Y = \sqrt{5}$, the matrix $\mathbf{D}_\mathrm{g}$ destabilizes the mode with the higher frequency, whereas the matrix $\mathbf{D}_\mathrm{r}$ makes unstable the mode with the lower frequency (cf. figure 2*b*). Figure 3 compares the real and imaginary parts of the eigenvalues λ depending on Y for the matrices $\mathbf{D}$ corresponding to the red and green compartments of the stability domain shown in figure 2*a*, as well as to its tangent cone.

Concluding, we quote from Freitas *et al.* [4], who noticed that the dependence of the spectrum of $\mathbf{L}_1$ on the spectra of $\mathbf{K}$ and $\mathbf{D}$ 'is very non-trivial'. We have just demonstrated that these peculiarities are essentially described by the properties of the stability boundary in the vicinity of the EP and in particular by the tangent cone to the stability domain at the EP. In the following, we will show that in an even more complicated situation when the gyroscopic and non-conservative positional forces are taken into account, the eigenvalue behaviour can be described in a similar geometrical manner.

3. Gyroscopic system with damping and non-conservative positional forces

Consider a linear system with $n = 2$ degrees of freedom

$$\ddot{\mathbf{z}} + (\delta\mathbf{D} + \Omega\mathbf{J})\dot{\mathbf{z}} + (\mathbf{K} + \nu\mathbf{J})\mathbf{z} = 0, \tag{3.1}$$

where the dot stands for time differentiation, and the real matrix of potential forces is $\mathbf{K} = \mathbf{K}^\mathrm{T} < 0$. The real matrix $\mathbf{D} = \mathbf{D}^\mathrm{T}$ corresponds to the damping forces and the skew-symmetric matrix $\mathbf{J} = \left(\begin{smallmatrix} 0 & -1 \\ 1 & 0 \end{smallmatrix}\right)$ represents gyroscopic forces when it is pre-multiplied by the parameter Ω and non-conservative positional (or circulatory [38]) forces when the pre-factor is ν [27,39,40].

Seeking the solutions to equation (3.1) in the form $\mathbf{z} \sim \mathbf{u}\exp(\lambda t)$, we arrive at the eigenvalue problem for a matrix polynomial

$$\mathbf{L}_2(\lambda)\mathbf{u} := (\lambda^2 + (\delta\mathbf{D} + \Omega\mathbf{J})\lambda + \mathbf{K} + \nu\mathbf{J})\mathbf{u} = 0. \tag{3.2}$$

When $n = 2$, the Leverrier–Barnett algorithm [24] applied to $\mathbf{L}_2$ results in the characteristic polynomial

$$q(\lambda) = \lambda^4 + q_1\lambda^3 + q_2\lambda^2 + q_3\lambda + q_4, \tag{3.3}$$

with the coefficients

$$\left.\begin{aligned} &q_1 = \delta \mathrm{tr}\mathbf{D}, \quad q_2 = \mathrm{tr}\mathbf{K} + \delta^2 \det \mathbf{D} + \Omega^2, \\ &q_3 = \delta(\mathrm{tr}\mathbf{K}\mathrm{tr}\mathbf{D} - \mathrm{tr}\mathbf{K}\mathbf{D}) + 2\Omega\nu \quad \text{and} \quad q_4 = \det \mathbf{K} + \nu^2. \end{aligned}\right\} \tag{3.4}$$

When the damping and non-conservative positional forces are absent, i.e. $\delta = 0$ and $\nu = 0$, the system (3.1) is a conservative gyroscopic system. Then, equation (3.1) can be transformed to the form $\dot{\mathbf{x}} = \mathbf{A}\mathbf{x}$, where the matrix $\mathbf{A}$ obeys the Hamiltonian symmetry, $\mathbf{SAS} = \mathbf{A}^{\mathrm{T}}$, and [27]

$$\mathbf{A} = \begin{pmatrix} -\frac{1}{2}\Omega\mathbf{J} & \mathbf{I} \\ -\mathbf{K} - \frac{1}{4}\Omega^2\mathbf{I} & -\frac{1}{2}\Omega\mathbf{J} \end{pmatrix}, \quad \mathbf{S} = \begin{pmatrix} 0 & -\mathbf{I} \\ \mathbf{I} & 0 \end{pmatrix} \quad \text{and} \quad \mathbf{x} = \begin{pmatrix} \mathbf{z} \\ \dot{\mathbf{z}} + \frac{1}{2}\Omega\mathbf{J}\mathbf{z} \end{pmatrix}, \tag{3.5}$$

where $\mathbf{I}$ is a unit 2×2 matrix. As a consequence, if λ is an eigenvalue of the gyroscopic system (equivalently, of the matrix $\mathbf{A}$), then so are its complex conjugate, $\bar{\lambda}$, and $-\lambda$. Therefore, the eigenvalues of the gyroscopic system are located symmetrically with respect to both real and imaginary axes of the complex plane.

Indeed, resolving equation (3.3) with $\delta = 0$ and $\nu = 0$ with respect to λ, we find that $\lambda = \pm \mathrm{i}\omega_{\pm}(\Omega)$, where

$$\omega_{\pm}(\Omega) = \sqrt{\omega_0^2 + \frac{\Omega_2}{2}(\sqrt{\Omega^2 - \Omega_2^2} \pm \sqrt{\Omega^2 - \Omega_1^2})\sqrt{\frac{\Omega^2}{\Omega_2^2} - 1}}. \tag{3.6}$$

The frequency $\omega_0 = \frac{1}{2}\sqrt{\Omega_2^2 - \Omega_1^2}$ is defined via the critical values of the gyroscopic parameter, $\Omega_{1,2}$, such that

$$0 \le \sqrt{-\kappa_2} - \sqrt{-\kappa_1} =: \Omega_1 \le \Omega_2 := \sqrt{-\kappa_1} + \sqrt{-\kappa_2}, \tag{3.7}$$

where $\kappa_2 < \kappa_1 < 0$ are eigenvalues of the matrix of potential forces $\mathbf{K}$.

Because $\mathbf{K} < 0$, the potential system without gyroscopic forces ($\Omega = 0$) is statically unstable, which corresponds to the two real positive eigenvalues λ and their two negative counterparts. With the increase in Ω, the real eigenvalues of the same sign move along the real axis in the complex plane towards each other until they merge at the EP at $\Omega = \Omega_1$ into the double real ones $\lambda = \pm\omega_0$. Increasing Ω further yields splitting of the double real eigenvalues into complex-conjugate pairs that start moving on the circle

$$(\mathrm{Re}\lambda)^2 + (\mathrm{Im}\lambda)^2 = \omega_0^2, \tag{3.8}$$

until they collide at another EP that exists at $\Omega = \Omega_2$, see black curves in figure 4*b*. When $\Omega > \Omega_2 > 0$, the gyroscopic system without damping and non-conservative positional forces is stable with four simple pure imaginary eigenvalues $\lambda = \pm\mathrm{i}\omega_{\pm}(\Omega)$, where the frequencies $0 < \omega_-(\Omega) < \omega_+(\Omega)$ are given by equation (3.6). This is a well-known phenomenon of gyroscopic stabilization of a statically unstable potential system by fast rotation [41].

With each of the pure imaginary eigenvalues, $\lambda = \pm\mathrm{i}\omega_{\pm}(\Omega)$ of the conservative gyroscopically stabilized system, an invariant known as the Krein or symplectic signature, is associated, $\mathrm{sign}(\mathrm{i}\omega_{\pm})$ [42],

$$\mathrm{sign}(\mathrm{i}\omega_{\pm}) := \mathrm{sgn}(\mathrm{i}\bar{\mathbf{w}}_{\pm}^{\mathrm{T}}\mathbf{S}\mathbf{w}_{\pm}), \tag{3.9}$$

where $\mathbf{w}_{\pm}$ are the eigenvectors of the matrix $\mathbf{A}$ at the eigenvalues $\mathrm{i}\omega_{\pm}(\Omega)$. Calculating the eigenvectors and substituting them into equation (3.9), we find

$$\mathrm{i}\bar{\mathbf{w}}_{\pm}^{\mathrm{T}}\mathbf{S}\mathbf{w}_{\pm} = \pm F^{\mp}(\Omega)\omega_{\pm}(\Omega)\sqrt{\Omega^2 - \Omega_2^2}\sqrt{\Omega^2 - \Omega_1^2}, \tag{3.10}$$

where

$$F^{\mp}(\Omega) = \frac{4k_{11} - (\sqrt{\Omega^2 - \Omega_1^2} \mp \sqrt{\Omega^2 - \Omega_2^2})^2}{2(\Omega^2 k_{11} + k_{12}^2)}, \tag{3.11}$$

and k_{11} and k_{12} are the entries of the matrix $\mathbf{K}$. When $\Omega > \Omega_2$, the sign of the right-hand side of equation (3.10) depends only on the sign of the functions $F^+(\Omega)$ and $F^-(\Omega)$. In the limit

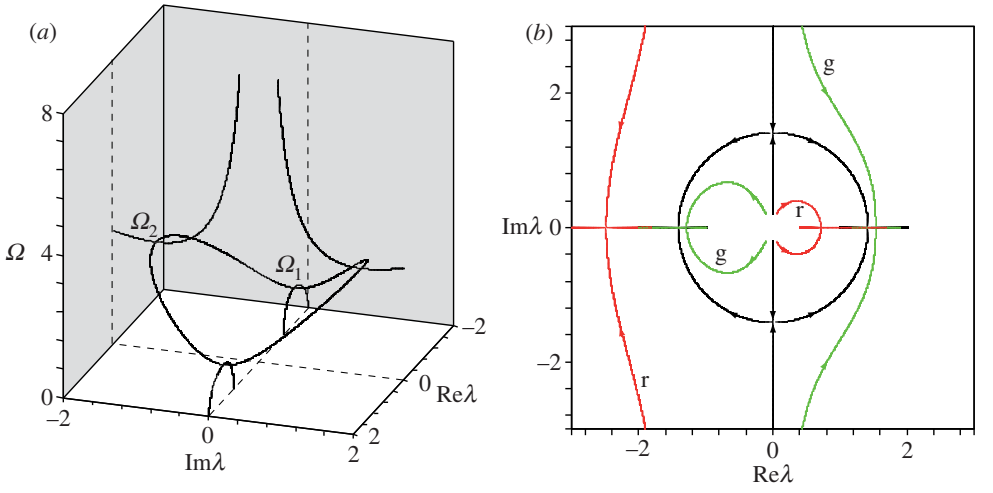

Figure 4. For $\kappa_1 = -1, \kappa_2 = -4$, tr$\mathbf{D} = 3$, tr$\mathbf{KD} = -6$, and det $\mathbf{D} = 1$: movement of eigenvalues (*a*) in the (Reλ, Imλ, Ω) space and (*b*) in the complex plane when Ω decreases from 10 to 0 and (black) $\delta = 0$ and $\nu = 0$, (red, r) $\delta = 1$ and $\nu = 0$, and (green, g) $\delta = 0$ and $\nu = 1$. (Online version in colour.)

$\Omega \to \infty$, we have $F^{\mp}(\Omega) \sim 2/\Omega^2 > 0$, and thus sign$(\mathrm{i}\omega_{\pm}(\Omega \to \infty)) = \pm 1$. Because the eigenvalues remain simple and pure imaginary on the whole interval $\Omega \in (\Omega_2, \infty)$ and the Krein signature is an invariant of an eigenvalue, we have sign$(\mathrm{i}\omega_{\pm}(\Omega)) = \pm 1$ for all $\Omega \in (\Omega_2, \infty)$. Note that sign$(-\mathrm{i}\omega_{\pm}) = -$sign$(\mathrm{i}\omega_{\pm})$.

Therefore, the *lower* eigenfrequency, ω_-, of the conservative gyroscopic system under study acquires a *negative* Krein signature, whereas the *higher* eigenfrequency, ω_+, has a *positive* Krein signature when Ω is within the interval of gyroscopic stabilization, $\Omega > \Omega_2 > 0$. The signature coincides with the sign of the energy of a mode with a given eigenfrequency $\omega_{\pm} > 0$ [42,43]. Passing through a non-semisimple 1 : 1 resonance, at $\Omega = \Omega_2$ when Ω is decreasing, is thus accompanied by merging of the two eigenvalues, one with a positive and another with a negative energy sign (Krein signature), which is known as the Krein collision [44], see black curves in figure 4.

How do the damping and non-conservative positional forces affect the pure imaginary eigenvalues $\mathrm{i}\omega_{\pm}(\Omega)$ of the gyroscopically stabilized conservative system? Does the Krein signature of the eigenvalues play a part?

The answer follows from the Taylor expansions of the eigenvalues of the perturbed gyroscopic system with respect to the parameters δ and ν. Indeed, if $\mathrm{i}\omega_{\pm}(\Omega)$ is a simple root of the characteristic polynomial (3.3) at $\delta = 0$ and $\nu = 0$, then the first-order correction to this root is [45]

$$\lambda(\delta, \Omega, \nu) = \mathrm{i}\omega_{\pm}(\Omega) - \delta \frac{\partial_{\delta} q(\Omega)}{\partial_{\lambda} q(\Omega)} - \nu \frac{\partial_{\nu} q(\Omega)}{\partial_{\lambda} q(\Omega)} + o(\delta, \nu), \tag{3.12}$$

where the derivatives are taken at $\delta = 0$ and $\nu = 0$. Taking into account that

$$2\omega_0^2 - 2\omega_{\pm}^2 + \Omega^2 - \Omega_2^2 = \mp\sqrt{\Omega^2 - \Omega_2^2}\sqrt{\Omega^2 - \Omega_1^2}, \tag{3.13}$$

from equation (3.12), we obtain in the linear approximation

$$\lambda(\delta, \Omega, \nu) = \mathrm{i}\omega_{\pm}(\Omega) \pm \nu \frac{\Omega}{\sqrt{\Omega^2 - \Omega_2^2}\sqrt{\Omega^2 - \Omega_1^2}} \mp \delta \frac{(\omega_{\pm}^2(\Omega) - \omega_0^2)\mathrm{tr}\mathbf{D} + 2\Omega_2\gamma_*}{2\sqrt{\Omega^2 - \Omega_2^2}\sqrt{\Omega^2 - \Omega_1^2}}, \tag{3.14}$$

where

$$\gamma_* = \frac{\mathrm{tr}\mathbf{KD} + (\Omega_2^2 - \omega_0^2)\mathrm{tr}\mathbf{D}}{2\Omega_2}. \tag{3.15}$$

Therefore, when $\Omega > \Omega_2 > 0$, the *non-conservative positional forces* with $\nu > 0$ *stabilize the negative energy mode*, $\mathrm{i}\omega_-(\Omega)$, but *destabilize the mode with the positive Krein signature*, $\mathrm{i}\omega_+(\Omega)$, see green curves in figure 4*b*.

The effect of damping forces depends on the structure of both the damping matrix $\mathbf{D}$ and the matrix $\mathbf{K}$ of potential forces.

When $\Omega > \Omega_2 > 0$, the *damping forces* with $\delta > 0$ *destabilize the negative energy mode*, $\mathrm{i}\omega_-(\Omega)$, and *stabilize the positive energy mode*, $\mathrm{i}\omega_+(\Omega)$, if

$$(A) : (\omega_\pm^2(\Omega) - \omega_0^2)\mathrm{tr}\mathbf{D} + 2\Omega_2\gamma_* > 0. \tag{3.16}$$

Otherwise, if

$$(B) : (\omega_\pm^2(\Omega) - \omega_0^2)\mathrm{tr}\mathbf{D} + 2\Omega_2\gamma_* < 0, \tag{3.17}$$

damping stabilizes the negative energy mode of the gyroscopically stabilized conservative system under study; *it can destabilize the positive energy mode* when $\Omega_2 < \Omega < \Omega_{\mathrm{cr}} < \infty$.

Examples of matrices $\mathbf{K}$ and $\mathbf{D}$ that satisfy condition (3.16) are given by

$$\mathbf{K}_A = \begin{pmatrix} -1 & 0 \\ 0 & -4 \end{pmatrix} \quad \text{and} \quad \mathbf{D}_{A_1} = \begin{pmatrix} 2 & 1 \\ 1 & 1 \end{pmatrix}. \tag{3.18}$$

Then, $\Omega_1 = 1$, $\Omega_2 = 3$, $\omega_0 = \sqrt{2}$ and $\gamma_* = \frac{5}{2}$. The eigenvalues of the matrix $\mathbf{D}_{A_1}$ are $\delta_{1,2} = (3 \pm \sqrt{5})/2 > 0$. Red (r) curves in figure 4*b* show the effect of the full dissipation with the positive definite matrix $\mathbf{D}_{A_1}$.

The destabilizing effect of damping forces with full dissipation on the negative energy modes of a stable Hamiltonian system is well known [46–48]. In hydrodynamics, this phenomenon manifests itself in connection, e.g. with the Kelvin–Helmholtz instability [49,50], stability of a boundary layer over a flexible surface [51–53] and Benjamin–Feir instability [42].

An interesting fact following from equation (3.16) is that the same effect can also be produced by the indefinite damping. Indeed, taking, e.g. $\mathbf{D} = \mathbf{D}_{A_2}$ with

$$\mathbf{D}_{A_2} = \begin{pmatrix} 1 & 2 \\ 2 & 1 \end{pmatrix} \tag{3.19}$$

and $\mathbf{K} = \mathbf{K}_A$ as in the above example, we find that the eigenvalues of the indefinite matrix $\mathbf{D}_{A_2}$ are $\delta_1 = -1$ and $\delta_2 = 3$, and $\gamma_* = \frac{3}{2}$. Hence, with $\mathbf{K} = \mathbf{K}_A$ and $\mathbf{D} = \mathbf{D}_{A_2}$, the inequality (3.16) is fulfilled for all $\Omega > \Omega_2 = 3$. Red (r) curves in figure 5*a* show how the positive energy modes are stabilized, and the negative energy modes are destabilized by the indefinite damping matrix $\mathbf{D}_{A_2}$.

However, indefinite damping can act inversely in comparison with the earlier described effect by stabilizing the negative energy mode and destabilizing the positive energy mode for Ω sufficiently close to Ω_2, see red (r) curves in figure 5*b*. They are plotted for the matrices

$$\mathbf{K}_B = \begin{pmatrix} -2 & 1 \\ 1 & -2 \end{pmatrix} \quad \text{and} \quad \mathbf{D}_B = \begin{pmatrix} 1 & -6 \\ -6 & 1 \end{pmatrix}, \tag{3.20}$$

with which the inequality (3.17) is satisfied in the case of $\omega_-(\Omega)$ for all $\Omega > \Omega_2$ and in the case of $\omega_+(\Omega)$ for $\Omega_2 < \Omega < \Omega_{\mathrm{cr}} < \infty$.

As was established in Kirillov [54,55], destabilization of the positive energy modes of a Hamiltonian system by indefinite damping or non-conservative positional forces is a basic mechanism leading to the onset of oscillatory instabilities induced by friction applied to rotating or moving continua [21] such as the singing wine glass [19,20] or a squealing disc brake [56,57], see Chen & Bogy [58], Ono *et al*. [59], Yang & Hutton [60] and Spelsberg-Korspeter *et al*. [61] for further mechanical examples, and see Kirillov *et al*. [62] for an example of a similar effect in magnetohydrodynamics.

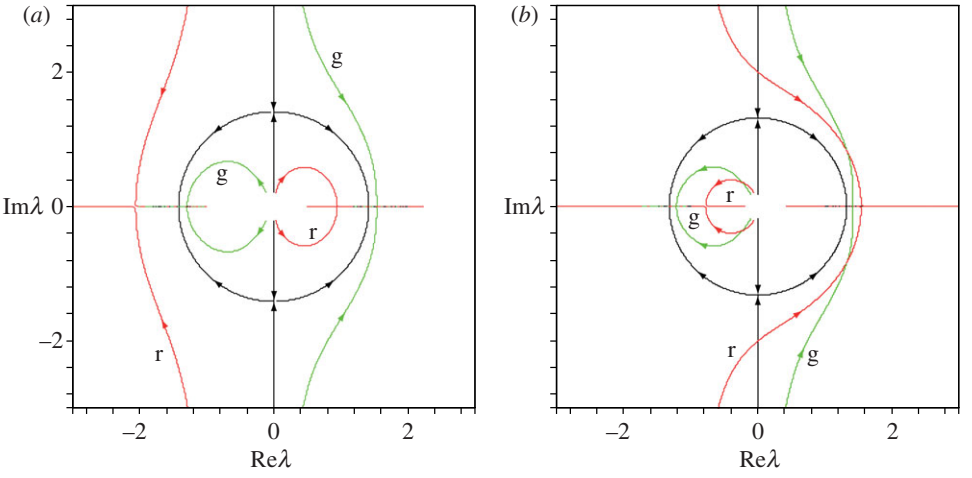

Figure 5. (*a*) For $\kappa_1 = -1$, $\kappa_2 = -4$, tr$\mathbf{D} = 2$, tr$\mathbf{KD} = -5$ and det $\mathbf{D} = -3$ and (*b*) for $\kappa_1 = -1$, $\kappa_2 = -3$, tr$\mathbf{D} = 2$, tr$\mathbf{KD} = -16$ and det $\mathbf{D} = -35$: movement of eigenvalues in the complex plane when Ω decreases from 10 to 0 and (black) $\delta = 0$ and $\nu = 0$, (red, r) $\delta = 1$ and $\nu = 0$, and (green, g) $\delta = 0$ and $\nu = 1$. (Online version in colour.)

From equation (3.14), a linear approximation follows to the boundary of the domain of asymptotic stability in the (δ, ν, Ω) space,

$$\nu = \frac{\Omega_2}{\Omega}\left[\gamma_* + \frac{\mathrm{tr}\mathbf{D}}{2}\frac{(\omega_\pm^2(\Omega) - \omega_0^2)}{\Omega_2}\right]\delta. \tag{3.21}$$

In the vicinity of $\Omega = \Omega_2$, we have $\omega_\pm^2(\Omega) - \omega_0^2 \simeq \pm\omega_0\sqrt{2\Omega_2(\Omega - \Omega_2)}$. Taking this into account in equation (3.21), we find a simple approximation to the gyroscopic parameter Ω near the EP $(0, 0, \Omega_2)$ at the threshold of the gyroscopic stabilization [27,63],

$$\Omega = \Omega_2 + \Omega_2\frac{2}{(\omega_0\mathrm{tr}\mathbf{D})^2}\left(\frac{\nu}{\delta} - \gamma_*\right)^2 + o\left(\frac{\nu}{\delta} - \gamma_*\right)^2. \tag{3.22}$$

Again, we have obtained an equation that is in the familiar canonical form for the Whitney umbrella surface: $Y = X^2/Z^2$. Hence, at the EP $(0, 0, \Omega_2)$, the boundary of the domain of gyroscopic stabilization in the presence of damping and non-conservative forces has the Whitney umbrella singularity [63], see figure 6*a*. In the first approximation with respect to δ and ν, the stability boundary is a ruled surface, i.e. a set of points swept by moving straight lines given by equation (3.21) that all intersect the Ω-axis orthogonally. At $\Omega = \Omega_2$, the lines degenerate and merge into one,

$$\nu = \gamma_*\delta. \tag{3.23}$$

In the (δ, ν, Ω) space, a part of the plane (3.23) limited by the inequalities $\Omega > \Omega_2$ and $\delta > 0$ constitutes a tangent cone [34,35] to the domain of gyroscopic stabilization at the EP $(0, 0, \Omega_2)$.

In the vicinity of the EP, it is the tangent cone to the stability domain that determines the transition of instability from the modes with negative Krein signature to that with the positive one. Indeed, as was shown by Kirillov [36,64], perturbation of the double eigenvalue $i\omega_0$ at the EP yields the following approximation of the trajectories of the perturbed simple eigenvalues in the complex plane

$$\left(\mathrm{Im}\lambda - \omega_0 - \mathrm{Re}\lambda - \frac{a}{2}\right)^2 - \left(\mathrm{Im}\lambda - \omega_0 + \mathrm{Re}\lambda + \frac{a}{2}\right)^2 = 2d, \tag{3.24}$$

where $a := -\omega_0\langle\mathbf{h}, \mathbf{p}\rangle$, $d := \omega_0\langle\mathbf{f}, \mathbf{p}\rangle$, the angular brackets denote the scalar product in $\mathbb{R}^2$ of the vector of parameters $\mathbf{p}^{\mathrm{T}} = (\delta, \nu)$, and the real vectors $\mathbf{f}^{\mathrm{T}} = (f_\delta, f_\nu)$ and $\mathbf{h}^{\mathrm{T}} = (h_\delta, h_\nu)$ with

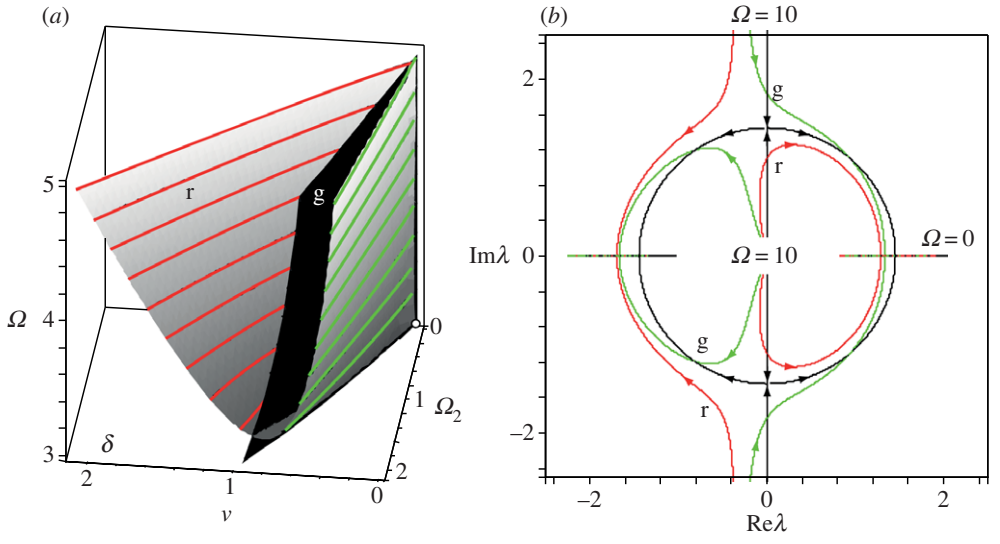

Figure 6. For $\kappa_1 = -1$, $\kappa_2 = -4$, tr$\mathbf{D} = 3$, tr$\mathbf{KD} = -6$ and det $\mathbf{D} = 1$: (*a*) the boundary of the domain of asymptotic stability with the Whitney umbrella singularity at the EP (0, 0, $\Omega_2 = 3$) in the (δ, ν, Ω) space and (black) the switching surface (3.28); (*b*) movement of eigenvalues in the complex plane when Ω decreases from 10 to 0 and (black) $\delta = 0$ and $\nu = 0$, (red, r) $\delta = 0.3$ and $\nu = 0.6$, and (green, g) $\delta = 0.3$ and $\nu = 0.9$. (Online version in colour.)

components that are expressed by means of the derivatives of the characteristic polynomial $q(\lambda)$ as [45]

$$f_s := \frac{2}{\mathrm{i}\omega_0}\frac{\partial_{p_s} q}{\partial_\lambda^2 q}, \quad h_s := \frac{2}{\omega_0}\frac{2\alpha_0(\mathrm{i}\omega_0)^{-1}\partial_{p_s} q - \partial^2_{\lambda p_s} q}{\partial_\lambda^2 q} \quad \text{and} \quad \alpha_0 = \mathrm{i}\omega_0 \frac{1}{3}\frac{\partial_\lambda^3 q}{\partial_\lambda^2 q}, \tag{3.25}$$

which should be evaluated at the EP. Then,

$$\alpha_0 = 1, \quad f_\delta = \frac{\Omega_2}{2\omega_0^2}\gamma_*, \quad f_\nu = -\frac{\Omega_2}{2\omega_0^2}, \quad h_\delta = \frac{\Omega_2\gamma_* - \omega_0^2 \mathrm{tr}\mathbf{D}}{2\omega_0^3} \quad \text{and} \quad h_\nu = -\frac{\Omega_2}{2\omega_0^3}, \tag{3.26}$$

and finally,

$$a = \frac{\mathrm{tr}\mathbf{D}}{2}\delta \quad \text{and} \quad d = \frac{\Omega_2}{2\omega_0}(\gamma_*\delta - \nu). \tag{3.27}$$

Note that in the final expression (3.27) for the coefficient a, the degeneration condition (3.23) has been taken into account [36].

Therefore, in the close vicinity of the EP, the movement of the perturbed eigenvalues in the complex plane is well approximated by the branches of a hyperbola (3.24), which are shifted off the imaginary axis to the left by a quantity $\delta \mathrm{tr}\mathbf{D}/4$. It is clear that when $\gamma_*\delta - \nu > 0$, i.e. when 'dissipation prevails', the eigenvalue with the lower frequency (negative energy mode) becomes unstable, see the r curves in figure 6*b*. If $\gamma_*\delta - \nu < 0$, which happens either when 'non-conservative positional forces prevail' in the perturbation or when specific forms of indefinite damping are used, the instability transfers to the mode with the higher frequency (positive energy mode), see g curves in figure 6*b*. Hence, the tangent cone to the stability domain in the (δ, ν, Ω) space at the EP gives a linear approximation to a surface (shown in black in figure 6*a*) that subdivides the stability domain into two compartments (marked by green (g) and red (r) level curves in figure 6*a*) that correspond to destabilization of either negative energy modes (r) or positive energy modes (g) of the stable gyroscopic system (figure 6*b*).[2]

The full stability boundary determined by equation $q_1q_2q_3 - q_1^2q_4 - q_3^2 = 0$ following from the Routh–Hurwitz conditions applied to the polynomial (3.3) is shown in figure 6*a*. It is a quadratic

[2]Cf. the eigencurves of fast and slow precession plotted in Samantaray *et al*. [65] for the Crandall gyropendulum [41,66].

equation with respect to ν that yields two sheets of the stability boundary that are connected to each other when the discriminant of the quadratic equation vanishes. This yields an equation of the surface

$$\nu = \delta\Omega \frac{\delta^2 \mathrm{tr}\mathbf{D}\,\det\mathbf{D} + 4\Omega_2\gamma_* + \mathrm{tr}\mathbf{D}(\Omega^2 - \Omega_2^2)}{\delta^2(\mathrm{tr}\mathbf{D})^2 + 4\Omega^2}, \tag{3.28}$$

which is shown in black in figure 6*a*. The linear approximation to this surface at the EP is the plane (3.23) that contains a tangent cone to the stability domain. When the parameters are in the g compartment of the stability domain with respect to this surface, the eigenvalue with a higher frequency has a smaller negative real part, whereas inside the r compartment, it is the eigenvalue with the lower frequency that is less stable. Consequently, when parameters are varied in such a manner that the stability boundary is penetrated from the green (g) side, the high-frequency mode is unstable. If this happens from the red (r) side, then the lower frequency mode is destabilized.

Therefore, the Krein signature of pure imaginary eigenvalues of the stable gyroscopic (Hamiltonian) system manifests itself deeply inside the parameter region of the dissipative system. In the first approximation, it is the tangent cone to the stability boundary at the EP associated with the Whitney umbrella singularity that separates the parameter sets destabilizing either negative- or positive-energy modes. The former are made unstable either by full dissipation or by a specific indefinite damping prescribed by equation (3.16), whereas the latter needs either non-conservative positional forces or another specific type of indefinite damping determined by equation (3.17) to be unstable.

Therefore, as figure 6*a* demonstrates, such physically different phenomena as, for example, the modulational instability in hydrodynamics and friction-induced instability in rotor dynamics live, in fact, not very far from each other under the same roof of a unique Whitney umbrella, being, however, separated by the 'switching surface' that reduces to the tangent cone to the stability domain at the singular EP of its stability boundary.

4. Example: Benjamin–Feir modulational instability

As an example that can be treated both as the Hamiltonian system perturbed by dissipation and as a $\mathcal{PT}$-symmetric indefinitely damped gyroscopic system perturbed by non-conservative positional and additional damping forces, we consider the effect of enhancement of the Benjamin–Feir modulational instability with dissipation first described by Bridges & Dias [42].

A monochromatic plane wave with a finite amplitude propagating in a dispersive medium can be disintegrated into a train of short pulses when the amplitude exceeds some threshold [67]. This process develops owing to an unbounded increase in the percentage modulation of the wave, i.e. instability of the carrier wave with respect to modulations. This is fundamental for modern fluid dynamics, nonlinear optics and plasma physics *modulational instability*.[3]

Without dissipation, a slowly varying in time envelope A of the rapidly oscillating carrier wave is described by the NLS

$$\mathrm{i}A_t + \alpha A_{xx} + \gamma|A|^2A = 0, \tag{4.1}$$

which can be derived in the rotating wave approximation [67]. In equation (4.1), α and γ are positive real numbers, $\mathrm{i} = \sqrt{-1}$, and the modulations are restricted to one space dimension x. Equation (4.1) has a solution in the form of a monochromatic wave

$$A = A_0\mathrm{e}^{\mathrm{i}kx - \mathrm{i}\omega t}, \tag{4.2}$$

where the frequency of the modulation, ω, depends on the amplitude $A_0 = u_1^0 + \mathrm{i}u_2^0$ and spatial wavenumber k as

$$\omega = \alpha k^2 - \gamma\|\mathbf{u}_0\|^2, \tag{4.3}$$

with $\mathbf{u}_0^{\mathrm{T}} = (u_1^0, u_2^0)$ [42,70].

[3]Known as the *Benjamin–Feir instability* in hydrodynamics [68] and as the *Bespalov–Talanov instability* in nonlinear optics [69].

The modulational instability can be enhanced with additional dissipation [42]. Below, we interpret this effect in terms of the mutual location of $\mathcal{PT}$-symmetric gyroscopic systems with indefinite damping with respect to general dissipative ones.

Introducing into equation (4.1) dispersive and viscous losses with the coefficients a and b, respectively, we arrive at the dissipatively perturbed NLS

$$\mathrm{i}A_t + (\alpha - \mathrm{i}a)A_{xx} + \mathrm{i}bA + \gamma|A|^2A = 0. \tag{4.4}$$

Separating the real and imaginary parts of the complex amplitude $A = u_1 + \mathrm{i}u_2$, we rewrite equation (4.4) as [42]

$$\mathbf{J}\mathbf{u}_t + \alpha\mathbf{u}_{xx} + \gamma\|\mathbf{u}\|^2\mathbf{u} - a\mathbf{J}\mathbf{u}_{xx} + b\mathbf{J}\mathbf{u} = 0, \tag{4.5}$$

where $\mathbf{u}^{\mathrm{T}} = (u_1, u_2)$ and $\mathbf{J} = \left(\begin{smallmatrix} 0 & -1 \\ 1 & 0 \end{smallmatrix}\right)$. Assuming a solution to equation (4.5) in the form $\mathbf{u} = \mathbf{R}(\mathbf{u}_0 + \mathbf{z}(x,t))$, where

$$\mathbf{R} = \begin{pmatrix} \cos(kx - \omega t) & -\sin(kx - \omega t) \\ \sin(kx - \omega t) & \cos(kx - \omega t) \end{pmatrix} \tag{4.6}$$

and $\mathbf{z}$ is a perturbation to the travelling wave solution of the undamped NLS with the amplitude vector $\mathbf{u}_0$, we obtain a linearization of equation (4.5),

$$\mathbf{J}\mathbf{z}_t + 2\alpha k\mathbf{J}\mathbf{z}_x + \alpha\mathbf{z}_{xx} + 2\gamma\mathbf{u}_0\mathbf{u}_0^{\mathrm{T}}\mathbf{z} + ak^2\mathbf{J}\mathbf{z} + 2ak\mathbf{z}_x - a\mathbf{J}\mathbf{z}_{xx} + b\mathbf{J}\mathbf{z} = 0, \tag{4.7}$$

where the dyad $\mathbf{u}_0\mathbf{u}_0^{\mathrm{T}}$ is a 2×2 symmetric matrix. Note that we have taken into account the relation (4.3) and following Bridges & Dias [42] assumed that the dissipation is a second-order effect in a sense that the travelling wave exists for a sufficiently long time before the effects of dissipation become significant.

Looking for a solution to equation (4.7) that has a form $\mathbf{z}(x,t) \sim \mathbf{v}(t)\cos\sigma x + \mathbf{w}(t)\sin\sigma x$, we arrive at the two coupled equations

$$\left.\begin{aligned} &\mathbf{J}\dot{\mathbf{v}} + 2\alpha k\sigma\mathbf{J}\mathbf{w} - \alpha\sigma^2\mathbf{v} + 2\gamma\mathbf{u}_0\mathbf{u}_0^{\mathrm{T}}\mathbf{v} + 2ka\sigma\mathbf{w} + (a(\sigma^2{+}k^2){+}b)\mathbf{J}\mathbf{v} = 0 \\ \text{and}\quad &\mathbf{J}\dot{\mathbf{w}} - 2\alpha k\sigma\mathbf{J}\mathbf{v} - \alpha\sigma^2\mathbf{w} + 2\gamma\mathbf{u}_0\mathbf{u}_0^{\mathrm{T}}\mathbf{w} - 2ka\sigma\mathbf{v} + (a(\sigma^2{+}k^2){+}b)\mathbf{J}\mathbf{w} = 0. \end{aligned}\right\} \tag{4.8}$$

Note that equations (4.7) and (4.8) contain terms proportional to ak^2 that are missing in the corresponding equations derived in Bridges & Dias [42].

Differentiating the first of equations (4.8) once and using the second one in order to extract $\mathbf{w}$ and its derivative, we decouple the equation for the vector $\mathbf{v}$,

$$\begin{aligned} &\ddot{\mathbf{v}} + 2((a(\sigma^2 + k^2) + b)\mathbf{I} + q\mathbf{J})\dot{\mathbf{v}} + \mathbf{P}\mathbf{v} + ((a(\sigma^2 + k^2) + b)\mathbf{I} + q\mathbf{J})^2\mathbf{v} \\ &\quad - \frac{2\gamma(\alpha\mathbf{J} + a\mathbf{I})(\alpha\mathbf{J}\mathbf{D}(\dot{\mathbf{v}} + (b + ak^2)\mathbf{v}) + 2a\gamma\|\mathbf{u}_0\|^2\mathbf{u}_0\mathbf{u}_0^{\mathrm{T}}\mathbf{v})}{\alpha^2 + a^2} = 0, \end{aligned} \tag{4.9}$$

where $\mathbf{I}$ is a unit matrix, $q = \alpha\sigma^2 - \gamma\|\mathbf{u}_0\|^2$,

$$\mathbf{P} = \gamma^2\|\mathbf{u}_0\|^4\mathbf{I} - 4k^2\sigma^2(\alpha\mathbf{J} + a\mathbf{I})^2 \quad \text{and} \quad \mathbf{D} = \mathbf{u}_0\mathbf{u}_0^{\mathrm{T}}\mathbf{J} - \mathbf{J}\mathbf{u}_0\mathbf{u}_0^{\mathrm{T}}. \tag{4.10}$$

In the absence of dispersive and viscous losses, i.e. when $a = 0$ and $b = 0$, equation (4.9) reduces to the standard form [39]

$$\ddot{\mathbf{v}} + 2q\mathbf{J}\dot{\mathbf{v}} + 2\gamma\mathbf{D}\dot{\mathbf{v}} + (\mathbf{P}_0 + (q\mathbf{J})^2)\mathbf{v} = 0, \tag{4.11}$$

where $\mathbf{P}_0 = (\gamma^2\|\mathbf{u}_0\|^4 + 4\alpha^2k^2\sigma^2)\mathbf{I}$, see Kirillov [23].

Equation (4.11) describes a $\mathcal{PT}$-symmetric gyroscopic system with the indefinite damping matrix $\mathbf{D}$ [26]. The eigenvalues $\delta_{1,2}(\mathbf{D}) = \pm\|\mathbf{u}_0\|^2$ differ by sign only. This implies that the spectrum

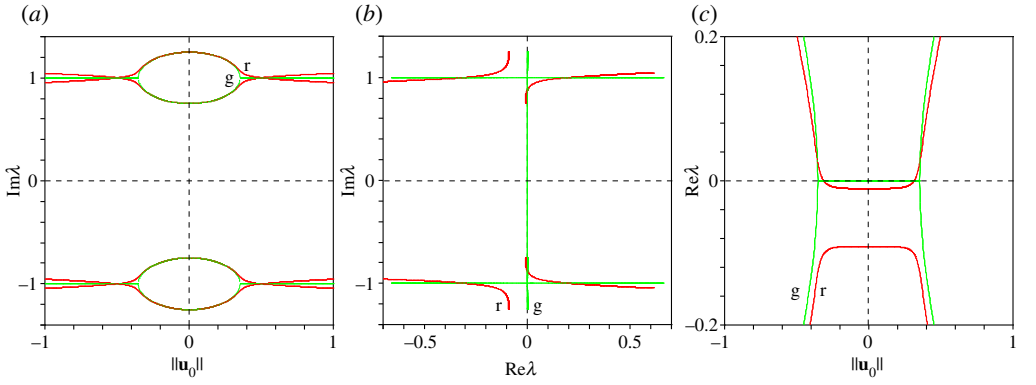

Figure 7. $\alpha = 1, k = 1, \sigma = 0.5, \gamma = 1$ and (green, g) $a = 0$ and $b = 0$ or (red, r) $a = 0.04$ and $b = 0.0008$: (*a*) frequency of the perturbation in dependence on $\|\mathbf{u}_0\|$; (*b*) movement of eigenvalues in the complex plane; (*c*) growth rates of the perturbation in the presence of dissipation (red, r) become positive at lower values of $\|\mathbf{u}_0\|$ than in the undamped case (green, g) (*dissipation-enhanced modulational instability*). (Online version in colour.)

of the system (4.11) is Hamiltonian. Indeed, the characteristic equation of the system (4.11)

$$\lambda^4 + 2\alpha\sigma^2(4\alpha k^2 + \alpha\sigma^2 - 2\gamma\|\mathbf{u}_0\|^2)\lambda^2 + \alpha^2\sigma^4(4\alpha k^2 - \alpha\sigma^2 + 2\gamma\|\mathbf{u}_0\|^2)^2 \tag{4.12}$$

determines the frequency and the growth rate of the perturbed modulation as

$$\lambda = \pm i2\alpha k\sigma \pm i\sigma\sqrt{2\alpha\gamma(\|\mathbf{u}_0\|_i^2 - \|\mathbf{u}_0\|^2)}, \tag{4.13}$$

where [42,71]

$$\|\mathbf{u}_0\|_i^2 = \frac{\alpha\sigma^2}{2\gamma}. \tag{4.14}$$

At small amplitudes of the modulation, the eigenvalues are pure imaginary. With an increase in the amplitude, the modes with the opposite Krein signature collide at the threshold $\|\mathbf{u}_0\| = \|\mathbf{u}_0\|_i$. At $\|\mathbf{u}_0\| > \|\mathbf{u}_0\|_i$, the double pure imaginary eigenvalue splits into complex-conjugate eigenvalues, one of which has a positive real part that corresponds to the modulational instability in the ideal (undamped) case, see green (g) curves in figure 7. Hence, the form of equation (4.11) suggests interpretation of the modulational instability as the destabilization of a $\mathcal{PT}$-symmetric gyroscopic system by indefinite damping [5,22].

The dispersive and viscous losses change the mechanism of the onset of the modulational instability as the evolution of eigenvalues shown by red (r) curves in figure 7 demonstrates. First, the eigenvalues do not merge into a double one anymore and simply pass in a close vicinity of each other, figure 7*b*. The modulational instability takes place when a pair of complex eigenvalues with a smaller absolute value of the imaginary part moves to the right in the complex plane. Second, the amplitude, $\|\mathbf{u}_0\|$, at the instability threshold can be lower than that in the undamped case, figure 7*c*. This is the effect of enhancement of the modulational instability with dissipation described by Bridges & Dias [42].

Writing the Routh–Hurwitz conditions for the characteristic polynomial of the system (4.8), which coincides with that of equation (4.9), we find the threshold of the modulational instability in the presence of dissipation

$$4\sigma^2a^2k^2\gamma^2\|\mathbf{u}_0\|^4 + 2\sigma^2\alpha\gamma r\|\mathbf{u}_0\|^2 - r((b + a(\sigma^2 + k^2))^2 + \alpha^2\sigma^4) = 0, \tag{4.15}$$

where $r = (b + a(\sigma^2 + k^2))^2 - 4a^2\sigma^2k^2$. The threshold (4.15) plotted in the $(a, b, \|\mathbf{u}_0\|)$ space is shown in figure 8*a*. The surface has a self-intersection along an interval of the $\|\mathbf{u}_0\|$ axis. At the points of this interval, the stability boundary is efficiently described by its linear approximation.

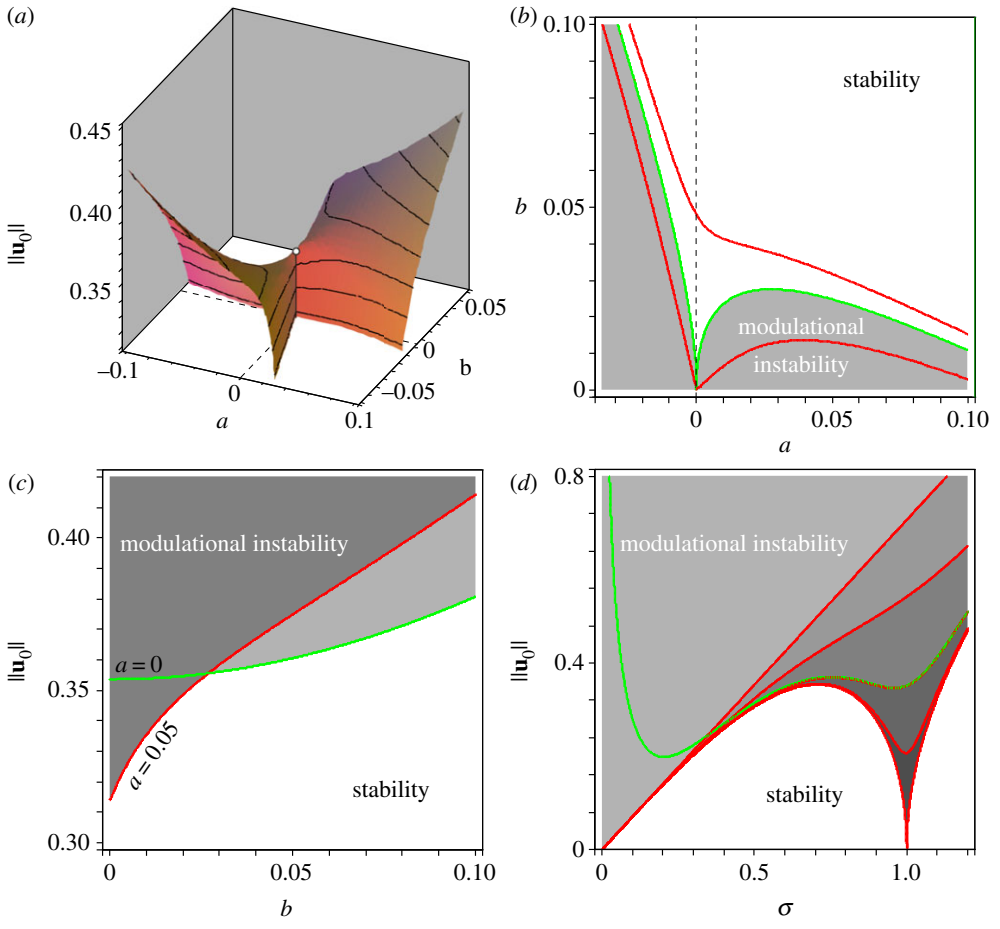

Figure 8. For $\alpha = 1$, $\gamma = 1$, and $k = 1$: (*a*) the threshold (4.15) at $\sigma = 0.5$; (*b*) its cross sections in the (a,b) plane at (lower curve) $\|\mathbf{u}_0\| = 0.34$, (intermediate curve) $\|\mathbf{u}_0\| = \|\mathbf{u}_0\|_i$ and (upper curve) $\|\mathbf{u}_0\| = 0.36$ and (*c*) in the $(b, \|\mathbf{u}_0\|)$ plane at $a = 0$ and $a = 0.05$; (*d*) in the $(\sigma, \|\mathbf{u}_0\|)$ plane, the threshold (4.15) in the limit $a \to 0$ for (straight red (dark) line) $\beta := a/b = 0$ and (subsequent lower red (dark) curves) $\beta = 5, 50, 500, \infty$ given by equation (4.16) and (4.19); the green (bright) curve is the threshold (4.15) at $a = 0.04$ and $b = 0.0008$. (Online version in colour.)

Indeed, resolving equation (4.15) with respect to b and expanding the solution in a, we find a linear approximation of the region of asymptotic stability in the (a, b) plane,

$$b = \left[-\sigma^2 - k^2 \pm \frac{k\sigma\,(2\|\mathbf{u}_0\|_i^2 - \|\mathbf{u}_0\|^2)}{\|\mathbf{u}_0\|_i \sqrt{\|\mathbf{u}_0\|_i^2 - \|\mathbf{u}_0\|^2}} \right] a + o(a). \tag{4.16}$$

The linear approximation (4.16) consists of two straight lines, the angle between which decreases when $\|\mathbf{u}_0\|$ approaches $\|\mathbf{u}_0\|_i$. At the EP $\|\mathbf{u}_0\| = \|\mathbf{u}_0\|_i$, the linear approximation (4.16) degenerates into a single line $a = 0$.

For $a \ll b$, equation (4.16) yields a simple estimate of the threshold of the dissipative modulational instability in the vicinity of the EP $(a, b, \|\mathbf{u}_0\|_i)$,

$$\|\mathbf{u}_0\|_d \simeq \|\mathbf{u}_0\|_i \left(1 - \frac{k^2\sigma^2}{2}\frac{a^2}{b^2}\right) \leq \|\mathbf{u}_0\|_i. \tag{4.17}$$

Equation (4.17) has the form $Y = X^2/Z^2$ that is canonical for the Whitney umbrella surface [30]. Therefore, as is visible in figure 8*a*, the instability threshold (4.15) indeed possesses the Whitney umbrella singularity at $a = 0$, $b = 0$ and $\|\mathbf{u}_0\| = \|\mathbf{u}_0\|_i$ in the $(a, b, \|\mathbf{u}_0\|)$ space.

The presence of the singularity on the stability boundary explains why at every small $a \neq 0$, there exists a domain of modulational instability at smaller values of $\|\mathbf{u}_0\|$ with respect to that for $a = 0$, figure 8*c*. This enhancement of the modulational instability with dissipation discussed in Bridges & Dias [42] is clearly seen in the approximation (4.17). On the other hand, some combinations of a and b yield positive increments to the stability domain shown in light grey in figure 8*c*. For example, at $\|\mathbf{u}_0\| = \|\mathbf{u}_0\|_i$, there exists a stability domain in the (a, b) plane that has a cuspidal point singularity at the origin, figure 8*b*. Quadratic approximation to the cusp follows from the expression (4.15) as

$$b = \sigma\sqrt{\sigma}\sqrt{\alpha k|a|} - a(\sigma^2 + k^2) + o(a). \tag{4.18}$$

Figure 8*d* demonstrates how the existence of the Whitney umbrella singularity at the EP influences the instability threshold in the $(\sigma, \|\mathbf{u}_0\|)$ plane. The straight red (dark) line in figure 8*d* is the undamped threshold (4.14) that yields $\|\mathbf{u}_0\| = \sigma\sqrt{\alpha/2\gamma}$; the green (bright) curve here shows the stability boundary (4.15) at $a = 0.04$ and $b = 0.0008$ so that $\beta := ab^{-1} = 50$. We see that the green (bright) line intersects the instability threshold in the undamped case, i.e. dissipation both increases and decreases the critical amplitude. However, when β is fixed and $a \to 0$, the stability boundary tends to a limiting curve that is below the undamped threshold for all $\sigma > 0$, and thus does not coincide with the line $\|\mathbf{u}_0\| = \sigma\sqrt{\alpha/2\gamma}$. This limiting curve is described by equation (4.16). In figure 8*d*, such limiting curves are plotted for $\beta = 5, 50, 500$ and for $\beta \to \infty$. In the latter case, equation (4.16) yields

$$\|\mathbf{u}_0\| = \pm\frac{\sigma}{k}\sqrt{\frac{\alpha}{2\gamma}(k^2 - \sigma^2)} \quad \text{and} \quad \|\mathbf{u}_0\| = \pm\sqrt{\frac{\alpha}{2\gamma}(\sigma^2 - k^2)}. \tag{4.19}$$

The curves (4.19) form a cusp at $\|\mathbf{u}_0\| = 0$ when $\sigma = k$, demonstrating a kind of resonance between the wavenumbers σ and k of the perturbation and modulation, figure 8*d*. Note however, that the modulational instability is characterized by $\sigma < k$ [42].

Therefore, enhancement of the modulational instability with dissipation is a manifestation of the effect of dissipation-induced instabilities [30,48] that occurs in a near $\mathcal{PT}$-symmetric gyroscopic system with indefinite damping.

5. Conclusion

We considered stability of a dissipative system in the vicinity of a $\mathcal{PT}$-symmetric indefinitely damped system as well as stability of a gyroscopic system perturbed by non-conservative positional and general damping forces with definite or indefinite matrices. In both cases, the spectrum of the ideal system has a Hamiltonian symmetry, i.e. the eigenvalues are situated symmetrically with respect to both real and imaginary axes of the complex plane. In both cases, the ideal system has a threshold in the parameter space (EP) whose violation yields instability via passing through the non-semisimple 1 : 1 resonance. We established that in both cases, the boundary of the domain of asymptotic stability has the Whitney umbrella singularity at the EP and a self-intersection along the interval of stability of the ideal system. We found that the tangent cone to the stability domain at the EP determines which mode becomes unstable under a perturbation. In the case of the gyroscopic system, we discovered that the modes with a negative Krein signature are destabilized by the full dissipation and some sort of indefinite damping, whereas the modes with a positive Krein signature are destabilized by non-conservative positional forces and another sort of indefinite damping. This classification has a clear geometrical picture in the parameter space. As an example that possesses both interpretations, an enhancement of the modulational instability with dissipation was studied in detail.

References

1. Freitas P. 1996 On some eigenvalue problems related to the wave equation with indefinite damping. *J. Diff. Equ.* **127**, 320–335. (doi:10.1006/jdeq.1996.0072)
2. Freitas P, Zuazua E. 1996 Stability results for the wave equation with indefinite damping. *J. Diff. Equ.* **132**, 338–353. (doi:10.1006/jdeq.1996.0183)
3. Chen G, Fulling SA, Narkowich FJ, Sun S. 1991 Exponential decay of energy of evolution equations with locally distributed damping. *SIAM J. Appl. Math.* **51**, 266–301. (doi:10.1137/0151015)
4. Freitas P, Grinfeld M, Knight PA. 1997 Stability of finite-dimensional systems with indefinite damping. *Adv. Math. Sci. Appl.* **7**, 437–448.
5. Freitas P. 1999 Quadratic matrix polynomials with Hamiltonian spectrum and oscillatory damped systems. *Z. Angew. Math. Phys.* **50**, 64–81. (doi:10.1007/s000330050139)
6. Schindler J, Li A, Zheng MC, Ellis FM, Kottos T. 2011 Experimental study of active LRC circuits with PT symmetries. *Phys. Rev. A* **84**, 040101(R). (doi:10.1103/PhysRevA.84.040101)
7. Bender CM, Boettcher S. 1998 Real spectra in non-Hermitian Hamiltonians having $\mathcal{PT}$-symmetry. *Phys. Rev. Lett.* **80**, 5243–5246. (doi:10.1103/PhysRevLett.80.5243)
8. Wang Q. 2004 Finite-dimensional $\mathcal{PT}$-symmetric Hamiltonians. *Czech. J. Phys.* **54**, 143–146. (doi:10.1023/B:CJOP.0000014379.56634.4f)
9. Bender CM, Mannheim PD. 2010 $\mathcal{PT}$ symmetry and necessary and sufficient conditions for the reality of energy eigenvalues. *Phys. Lett. A* **374**, 1616–1620. (doi:10.1016/j.physleta.2010.02.032)
10. Mostafazadeh A, Batal A. 2004 Physical aspects of pseudo-Hermitian and *PT*-symmetric quantum mechanics. *J. Phys. A, Math. Gen.* **37**, 11645–11679. (doi:10.1088/0305-4470/37/48/009)
11. Bender CM. 2007 Making sense of non-hermitian Hamiltonians. *Rep. Prog. Phys.* **70**, 947–1018. (doi:10.1088/0034-4885/70/6/R03)
12. Ruter CE, Makris KG, El-Ganainy R, Christodoulides DN, Segev M, Kip D. 2010 Observation of parity–time symmetry in optics. *Nat. Phys.* **6**, 192–195. (doi:10.1038/nphys1515)
13. Abdullaev FK, Kartashov YV, Konotop VV, Zezyulin DA. 2011 Solitons in PT-symmetric nonlinear lattices. *Phys. Rev. A* **83**, 041805. (doi:10.1103/PhysRevA.83.041805)
14. Driben R, Malomed, BA. 2011 Stability of solitons in parity–time-symmetric couplers. *Opt. Lett.* **36**, 4323–4325. (doi:10.1364/OL.36.004323)
15. Miroshnichenko AE, Malomed BA, Kivshar YS. 2011 Nonlinearly PT-symmetric systems: spontaneous symmetry breaking and transmission resonances. *Phys. Rev. A* **84**, 012123. (doi:10.1103/PhysRevA.84.012123)
16. Malomed BA, Winful HG. 1996 Stable solitons in two-component active systems. *Phys. Rev. E* **53**, 5365–5368. (doi:10.1103/PhysRevE.53.5365)
17. Atai J, Malomed BA. 1996 Stability and interactions of solitons in two-component systems. *Phys. Rev. E* **54**, 4371–4374. (doi:10.1103/PhysRevE.54.4371)
18. Figotin A, Vitebsky I. 2001 Spectra of periodic nonreciprocal electric circuits. *SIAM J. Appl. Math.* **61**, 2008–2035. (doi:10.1137/S0036139900370583)
19. Akay A. 2002 Acoustics of friction. *J. Acoust. Soc. Am.* **111**, 1525–1548. (doi:10.1121/1.1456514)
20. Spurr RT. 1961 The ringing of wine glasses. *Wear* **4**, 150–153. (doi:10.1016/0043-1648(61)90317-9)
21. Kroeger M, Neubauer M, Popp K. 2008 Experimental investigation on the avoidance of self-excited vibrations. *Phil. Trans. R. Soc. A* **366**, 785–810. (doi:10.1098/rsta.2007.2127)
22. Kliem W, Pommer C. 2009 Indefinite damping in mechanical systems and gyroscopic stabilization. *Z. Angew. Math. Phys.* **60**, 785–795. (doi:10.1007/s00033-007-7072-0)
23. Kirillov ON. 2011 Brouwer's problem on a heavy particle in a rotating vessel: wave propagation, ion traps, and rotor dynamics. *Phys. Lett. A* **375**, 1653–1660. (doi:10.1016/j.physleta.2011.02.056)
24. Barnett S. 1989 Leverrier's algorithm: a new proof and extensions. *SIAM J. Matrix Anal. Appl.* **10**, 551–556. (doi:10.1137/0610040)
25. Dietz B, Harney HL, Kirillov ON, Miski-Oglu M, Richter A, Schaefer F. 2011 Exceptional points in a microwave billiard with time-reversal invariance violation. *Phys. Rev. Lett.* **106**, 150403. (doi:10.1103/PhysRevLett.106.150403)
26. Kirillov ON. 2012 $\mathcal{PT}$-symmetry, indefinite damping and dissipation-induced instabilities. *Phys. Lett. A* **376**, 1244–1249. (doi:10.1016/j.physleta.2012.02.055)

27. Kirillov ON. 2007 Destabilization paradox due to breaking the Hamiltonian and reversible symmetry. *Int. J. Nonlinear Mech.* **42**, 71–87. (doi:10.1016/j.ijnonlinmec.2006.09.003)
28. Ziegler H. 1952 Die Stabilitaetskriterien der Elastomechanik. *Arch. Appl. Mech.* **20**, 49–56. (doi:10.1007/BF00536796)
29. Bottema O. 1956 The Routh–Hurwitz condition for the biquadratic equation. *Indag. Math.* **18**, 403–406.
30. Kirillov ON, Verhulst F. 2010 Paradoxes of dissipation-induced destabilization or who opened Whitney's umbrella? *Z. Angew. Math. Mech.* **90**, 462–488. (doi:10.1002/zamm.200900315)
31. Arnold VI. 1971 On matrices depending on parameters. *Russian Math. Surv.* **26**, 29–43. (doi:10.1070/RM1971v026n02ABEH003827)
32. Hoveijn I, Ruijgrok M. 1995 The stability of parametrically forced coupled oscillators in sum resonance. *Z. Angew. Math. Phys.* **46**, 384–392. (doi:10.1007/BF01003557)
33. Langford WF. 2003 Hopf meets Hamilton under Whitney's umbrella. In *IUTAM Symp. Nonlinear Stochastic Dynamics, Monticello, IL, USA, 26–30, August 2002* (eds SN Namachchivaya, YK Lin), Solid Mech. Appl. 110, pp. 157–165. Dordrecht, The Netherlands: Kluwer.
34. Levantovskii LV. 1980 The boundary of a set of stable matrices. *Usp Mat. Nauk* **35**, 212–214. (doi:10.1070/RM1980v035n02ABEH001651)
35. Levantovskii LV. 1982 Singularities of the boundary of a region of stability. *Funktsional. Anal. i Prilozhen.* **16**, 44–48, 96.
36. Kirillov ON. 2005 A theory of the destabilization paradox in non-conservative systems. *Acta Mech.* **174**, 145–166. (doi:10.1007/s00707-004-0194-y)
37. Krein MG. 1950 A generalization of several investigations of A. M. Liapunov on linear differential equations with periodic coefficients. *Dokl. Acad. Nauk SSSR* **73**, 445–448.
38. Ziegler H. 1953 Linear elastic stability. A critical analysis of methods. *Z. Angew. Math. Phys.* **4**, 89–121. (doi:10.1007/BF02067575)
39. Huseyin K. 1976 Standard forms of the eigenvalue problems associated with gyroscopic systems. *J. Sound Vibr.* **45**, 29–37. (doi:10.1016/0022-460X(76)90665-9)
40. Krechetnikov R, Marsden JE. 2006 On destabilizing effects of two fundamental non-conservative forces. *Physica D* **214**, 25–32. (doi:10.1016/j.physd.2005.12.003)
41. Crandall SH. 1995 The effect of damping on the stability of gyroscopic pendulums. *Z. Angew. Math. Phys.* **46**, S761–S780.
42. Bridges TJ, Dias F. 2007 Enhancement of the Benjamin–Feir instability with dissipation. *Phys. Fluids* **19**, 104104. (doi:10.1063/1.2780793)
43. MacKay RS. 1986 Stability of equilibria of Hamiltonian systems. In *Nonlinear phenomena and chaos* (ed. S Sarkar), pp. 254–270. Bristol, UK: Adam Hilger.
44. Morrison PJ. 1998 Hamiltonian description of the ideal fluid. *Rev. Mod. Phys.* **70**, 467–521. (doi:10.1103/RevModPhys.70.467)
45. Kirillov ON. 2007 On the stability of nonconservative systems with small dissipation. *J. Math. Sci.* **145**, 5260–5270. (doi:10.1007/s10958-007-0351-7)
46. MacKay RS. 1991 Movement of eigenvalues of Hamiltonian equilibria under non-Hamiltonian perturbation. *Phys. Lett. A* **155**, 266–268. (doi:10.1016/0375-9601(91)90480-V)
47. Maddocks JH, Overton ML. 1995 Stability theory for dissipatively perturbed Hamiltonian systems. *Commun. Pure Appl. Math.* **48**, 583–610. (doi:10.1002/cpa.3160480602)
48. Bloch AM, Krishnaprasad PS, Marsden JE, Ratiu TS. 1994 Dissipation induced instabilities. *Ann. de L'Inst. Henri Poincare. Anal. Non Lin.*, **11**, 37–90.
49. Fabrikant AL, Stepaniants YA. 1998 *Propagation of waves in shear flows*. Singapore: World Scientific.
50. Ostrovskii LA, Rybak SA, Tsimring LSh. 1986 Negative energy waves in hydrodynamics. *Sov. Phys. Usp.* **29**, 1040–1052. (doi:10.1070/PU1986v029n11ABEH003538)
51. Benjamin TB. 1963 The threefold classification of unstable disturbances in flexible surfaces bounding inviscid flows. *J. Fluid Mech.* **16**, 436–450. (doi:10.1017/S0022112063000884)
52. Carpenter PW, Davies C, Lucey AD. 2000 Hydrodynamics and compliant walls: does the dolphin have a secret? *Curr. Sci.* **79**, 758–765.
53. Landahl M. 1962 On the stability of a laminar incompressible boundary layer over a flexible surface. *J. Fluid Mech.* **13**, 609–632. (doi:10.1017/S002211206200097X)
54. Kirillov ON. 2008 Subcritical flutter in the acoustics of friction. *Proc. R. Soc. A* **464**, 2321–2339. (doi:10.1098/rspa.2008.0021)

55. Kirillov ON. 2009 Campbell diagrams of weakly anisotropic flexible rotors. *Proc. R. Soc. A* **465**, 2703–2723. (doi:10.1098/rspa.2009.0055)
56. Spurr RT. 1961 A theory of brake squeal. *Proc. Inst. Mech. Eng.* **1**, 33–52. (doi:10.1243/PIME_AUTO_1961_000_009_02)
57. Kinkaid NM, O'Reilly OM, Papadopoulos P. 2003 Automotive disc brake squeal. *J. Sound Vib.* **267**, 105–166. (doi:10.1016/S0022-460X(02)01573-0)
58. Chen J-S, Bogy DB. 1992 Mathematical structure of modal interactions in a spinning disk-stationary load system. *J. Appl. Mech.* **59**, 390–397. (doi:10.1115/1.2899532)
59. Ono K, Chen J-S, Bogy DB. 1991 Stability analysis for the head-disk interface in a flexible disk drive. *J. Appl. Mech.* **58**, 1005–1014. (doi:10.1115/1.2897675)
60. Yang L, Hutton SG. 1995 Interactions between an idealized rotating string and stationary constraints. *J. Sound Vib.* **185**, 139–154. (doi:10.1006/jsvi.1994.0368)
61. Spelsberg-Korspeter G, Kirillov ON, Hagedorn P. 2008 Modeling and stability analysis of an axially moving beam with frictional contact. *J. Appl. Mech.* **75**, 031001. (doi:10.1115/1.2755166)
62. Kirillov ON, Guenther U, Stefani F. 2009 Determining role of Krein signature for three-dimensional Arnold tongues of oscillatory dynamos. *Phys. Rev. E* **79**, 016205. (doi:10.1103/PhysRevE.79.016205)
63. Kirillov ON. 2007 Gyroscopic stabilization in the presence of nonconservative forces. *Dokl. Math.* **76**, 780–785. (doi:10.1134/S1064562407050353)
64. Kirillov ON. 2004 Destabilization paradox. *Dokl. Phys.* **49**, 239–245. (doi:10.1134/1.1753620)
65. Samantaray, AK, Bhattacharyya R, Mukherjee A. 2008 On the stability of Crandall gyropendulum. *Phys. Lett. A* **372**, 238–243. (doi:10.1016/j.physleta.2007.07.024)
66. Kirillov ON. 2006 Gyroscopic stabilization of non-conservative systems. *Phys. Lett. A* **359**, 204–210. (doi:10.1016/j.physleta.2006.06.040)
67. Kivshar YS, Peyrard M. 1992 Modulational instabilities in discrete lattices. *Phys. Rev. A* **46**, 3198–3207. (doi:10.1103/PhysRevA.46.3198)
68. Benjamin TB, Feir JE. 1967 Disintegration of wave trains on deep water. I. Theory. *J. Fluid Mech.* **27**, 417–430. (doi:10.1017/S002211206700045X)
69. Bespalov V, Talanov V. 1966 Filamentary structure of light beams in nonlinear liquids. *JETP Lett. USSR* **3**, 307–310.
70. Zakharov VE. 1968 Stability of periodic waves of finite amplitude on the surface of a deep fluid. *J. Appl. Mech. Tech. Phys.* **9**, 190–194. (doi:10.1007/BF00913182)
71. Zakharov VE, Ostrovsky LA. 2009 Modulation instability: the beginning. *Phys. D, Nonlin. Phenom.* **238**, 540–548. (doi:10.1016/j.physd.2008.12.002)